Biochimica et Biophysica Acta 1827 (2013) 986–1002

Contents lists available at SciVerse ScienceDirect

Biochimica et Biophysica Acta

journal homepage: www.elsevier.com/locate/bbabio

Review

[NiFe] hydrogenases: A common active site for hydrogen metabolism under diverse conditions ☆

Hannah S. Shafaat, Olaf Rüdiger, Hideaki Ogata, Wolfgang Lubitz *

Max-Planck-Institut für Chemische Energiekonversion, D-45470 Mülheim an der Ruhr, Germany

ARTICLE INFO

Article history:
Received 25 September 2012
Received in revised form 6 December 2012
Accepted 26 January 2013
Available online 8 February 2013

Keywords:
Oxygen-tolerant
Hydrogen
Spectroscopy
Electrochemistry
Renewable energy

ABSTRACT

Hydrogenase proteins catalyze the reversible conversion of molecular hydrogen to protons and electrons. The most abundant hydrogenases contain a [NiFe] active site; these proteins are generally biased towards hydrogen oxidation activity and are reversibly inhibited by oxygen. However, there are [NiFe] hydrogenase that exhibit unique properties, including aerobic hydrogen oxidation and preferential hydrogen production activity; these proteins are highly relevant in the context of biotechnological devices. This review describes four classes of these "nonstandard" [NiFe] hydrogenases and discusses the electrochemical, spectroscopic, and structural studies that have been used to understand the mechanisms behind this exceptional behavior. A revised classification protocol is suggested in the conclusions, particularly with respect to the term "oxygen-tolerance". This article is part of a special issue entitled: metals in bioenergetics and biomimetics systems.

1. Introduction

The energy problem facing the world today presents one of the greatest challenges in scientific research. The modern economy currently relies on the consumption of fossil fuels, which are becoming irreversibly depleted and has the concurrent effect of increasing CO_2 levels in the atmosphere. As the population and energy needs of the developing world are rising at a phenomenal rate [1], it is imperative that alternative, sustainable fuels are developed and implemented into everyday use. Towards that end, hydrogen has been proposed as one ecologically-friendly fuel for the future [2–4]. Hydrogen is a clean-burning fuel with high energy density, and as such, development of a "hydrogen economy" has become a target for many scientists and engineers. However, the current processes for generating large quantities of hydrogen are far from benign; high temperatures and pressures are used to combust natural gas over rare-earth or precious-metal catalysts, and CO_2 is generated along with hydrogen [5,6]. It is clear that the existing methods are not sustainable over the long term.

In contrast, nature has developed mild mechanisms to use hydrogen as a fuel [7,8]. Many different types of microbes, from strict anaerobes to obligate aerobes to photosynthetic bacteria, either produce or utilize hydrogen gas during their metabolic processes [8]. To accomplish this, specialized enzymes called hydrogenases have evolved. These metalloenzymes contain only nickel and iron, which are earth-abundant metals, and feature organometallic ligands, carbon monoxide and cyanide, that were previously unknown to exist in biological systems [9–11]. These enzymes function under ambient temperatures and pressures, with low overpotential, exhibit prolonged catalytic activity, and utilize water-derived protons for the synthesis of hydrogen with turnover frequencies of up to $10^4\ s^{-1}$; therefore, they are of great interest for biotechnological devices and bioinspired synthetic molecular catalysts, which currently suffer from limited stability and either low turnover frequencies or high overpotentials [12,13]. At this point, there are three main classes of hydrogenase protein, based on their active site metals: [FeFe], which contain only iron in their active site and are the fastest known biological catalysts for hydrogen oxidation/reduction; [NiFe], which possess a heterobimetallic active site; and [Fe]-only, which strictly couple hydrogen oxidation to substrate reduction [7,8,14–16]. A great deal of research has gone into understanding the catalytic cycle of each of these classes, and a powerful combination of spectroscopic, electrochemical, biological, theoretical, and structural techniques has provided great insight into the active site structure and dynamics of these systems (for recent reviews and reports, see refs. [8,17–22]). The general protein fold and active site structure of the [NiFe] hydrogenase are shown in Fig. 1.

Despite relatively good understanding of the catalytic mechanism, the use of hydrogenase proteins in biotechnological applications remains unfeasible [24–26]. There are a number of contributing factors to this point; one of the foremost remains extreme sensitivity to oxygen. Of the three classes known, the most robust towards oxygen are the [NiFe] proteins, which exhibit primarily reversible inactivation upon oxygen exposure; most [FeFe] proteins known to

☆ This article is part of a special issue entitled: metals in bioenergetics and biomimetics systems.

* Corresponding author. Tel.: +49 208 306 3614; fax: +49 208 306 3955.
E-mail address: wolfgang.lubitz@cec.mpg.de (W. Lubitz).

0005-2728/$ – see front matter © 2013 Elsevier B.V. All rights reserved.
http://dx.doi.org/10.1016/j.bbabio.2013.01.015

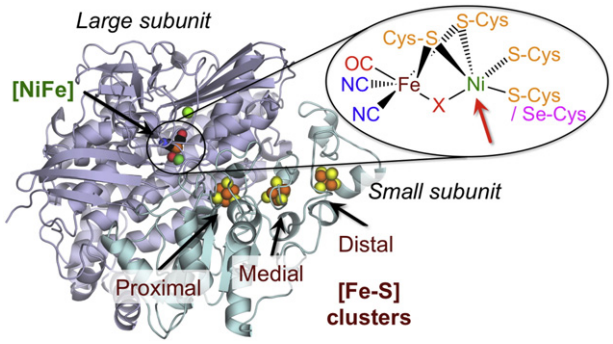

Fig. 1. Protein structure of the standard *Dv*MF [NiFe] hydrogenase (PDB: 1H2R) with [NiFe] active site, [4Fe-4S] proximal and distal clusters, and [3Fe-4S] medial cluster indicated. (*Inset*) The molecular structure of the active site [23]. The arrow indicates proposed H_2-binding site; the terminal cysteine that is replaced by selenocysteine is also shown.

date are extremely oxygen-sensitive. There are a number of shared traits associated with the well-studied, Group 1 [NiFe] hydrogenases. These proteins are ~100 kDa, multi-subunit proteins, located in the periplasmic space and often associated with a membrane. Many of these enzymes are unstable to a wide range of temperature or pH values. Because of the unusual organometallic ligands coordinated to the iron center, protein assembly requires many cofactors and thus heterologous expression is not trivial [27–29]. Finally, most [NiFe] hydrogenases function in nature primarily as hydrogen oxidation catalysts, which are ineffective in the context of proton reduction for hydrogen gas generation but remain of interest as catalysts for efficient hydrogen usage, for example, in fuel cells.

The above characteristics comprise what we will define as the "standard" [NiFe] hydrogenase. There is growing evidence, however, for a number of different types of naturally occurring, "nonstandard" [NiFe] hydrogenases [8,30–32]. With the exception of the Group 4 [NiFe] hydrogenases, which form part of the membrane-associated formate hydrogenlyase complexes that couple hydrogen production with energy conversion under strictly anaerobic conditions [8,33,34], many of these nonstandard enzymes display desirable characteristics, from oxygen tolerance to thermostability to a bias towards hydrogen production, in the context of alternative energy. Therefore they are thought to be superior candidates for implementation into biotechnological devices. Surprisingly, these nonstandard [NiFe] hydrogenases possess active sites that are nearly identical to the standard proteins, so it is not straightforward to identify which characteristics of the protein confer these specific features. Here, we describe four interesting classes of nonstandard [NiFe] hydrogenase—oxygen-tolerant membrane-bound hydrogenases, $NAD(P)^+$-reducing hydrogenases, regulatory hydrogenases, and [NiFeSe] hydrogenases—and for each class, attempt to describe the current level of understanding regarding the origin of their unique behavior. A short discussion on existing and future applications of these nonstandard hydrogenases is presented.

2. Oxygen-tolerant membrane-bound [NiFe] hydrogenases (O_2-tolerant MBHs)

Membrane-bound hydrogenases (MBHs) that are active under aerobic conditions have been isolated and characterized from many organisms; the most well-studied of these proteins include the Knallgas bacterium *Ralstonia eutropha* (*Re*) HoxGK, a closely-related Knallgas bacterium *Ralstonia metallodurans* (*Rm*), the aerobic thermophile *Aquifex aeolicus* (*Aa*) Hase I (which also has the interesting property of being unusually pH- and thermostable), and the enteric bacterium *Escherichia coli* (*Ec*) Hyd-1 proteins, though many more hydrogenases of this class are proposed to exist [32]. These proteins have been the subject of much research lately because they can oxidize hydrogen in the presence of oxygen, awarding them the title "oxygen-tolerant", which makes them of great interest for biotechnological or bioderived fuel cells [47]. As the terminology suggests, O_2-tolerant MBHs are coupled to the membrane and thus to the ubiquinone electron pool *via* protein–protein interactions between the small hydrogenase subunit (HoxK in *Re*) and an integral membrane *b*-type cytochrome protein (HoxZ in *Re*) that serves as the final electron transfer (ET) partner [48–50]. Both the *Aa* and *Re* O_2-tolerant MBHs can be isolated with or without this auxiliary ET protein [49,51], and hydrogenase activity, oxygen sensitivity, and spectroscopic properties seem relatively independent of the presence of this cytochrome [40,49,51].

2.1. Electrochemical studies of the O_2-tolerant MBHs reveal general catalytic properties

Protein film electrochemistry (PFE) has been extensively used in the study of hydrogenases [52,53]. This technique allows accurate electrochemical control of redox active enzymes immobilized on electrodes. In the case of hydrogenases, electrons are part of the catalytic reaction, so the measured current generated by the enzyme on the electrode in the presence of substrate gives a direct measurement of the turnover frequency of the enzyme (Fig. 3A and B). Combining this redox control on the enzyme with other experimental conditions, such as pH, substrate/inhibitor concentrations, and temperature, provides valuable information that is complementary to spectroscopic and crystallographic observations [52]. Moreover, because measurement of H_2 oxidation activity in the presence of O_2 is not possible using redox mediators [54], PFE is an excellent, highly accurate tool with which to study the oxygen tolerance of hydrogenases under catalytic conditions [52,53].

In general, oxygen-tolerant hydrogenases can be described as the hydrogenases that can maintain H_2 oxidation and/or H^+ reduction in the presence of O_2. Fig. 3C shows how a standard, oxygen-sensitive [NiFe] hydrogenase (*Dv*MF) becomes very rapidly inactivated by O_2 [55]. The catalytic current is not recovered after O_2 is flushed out of the cell by H_2; only a reductive potential step can partially reactivate the enzyme [56]. On the other hand, the oxygen-tolerant Hase I from *Aa* is not completely inactivated by O_2, and the current is recovered once O_2 leaves the electrochemical cell without requiring a more reductive potential step (Fig. 3D). Electrochemical PFE studies on O_2-tolerant MBHs in the last years have revealed specific features found to be common to all enzymes of this class.

The first general observation made about the O_2-tolerant MBHs was that they appeared to be unidirectional, H_2-uptake only hydrogenases. The *Aa* Hase I, *Ec* Hyd-1, and *Salmonella* O_2-tolerant MBHs show negligible H^+ reduction catalytic currents at negative potentials [31,58], indicating that these enzymes are completely biased towards H_2 oxidation, and only small H^+ reduction currents were measured for the O_2-tolerant MBHs from *Re* and *Rm* under 100% N_2 [31,40,47,58]. The catalytic currents for hydrogen oxidation were sustained even in the presence of 2% O_2, showing that O_2 was a weaker inhibitor than H_2 and CO [59]. In *Ec*, the unidirectional character of Hyd-1 can be understood with respect to overall metabolism of the organism because in addition to the oxygen-tolerant Hyd-1, *Ec* has another membrane-bound, oxygen-sensitive hydrogenase, Hyd-2. Under conditions of slow growth and fluctuating O_2 concentrations, Hyd-1 scavenges H_2 to generate a proton gradient through the coupled transmembrane *cyt b* subunit (HyaC). Reverse electron transport from the membrane-associated quinol pool at low potentials would collapse this transmembrane electrochemical gradient, indicating that the unidirectional character of Hyd-1 is an important physiological feature. Hyd-2, on the other hand is not coupled to a transmembrane HyaC-type quinone reductase. Instead, it exchanges electrons with the quinone pool without altering the proton gradient, allowing a release of electrons if the quinone/quinol pool becomes overreduced [58]. A similar survival mechanism may be at play in the other organisms [31].

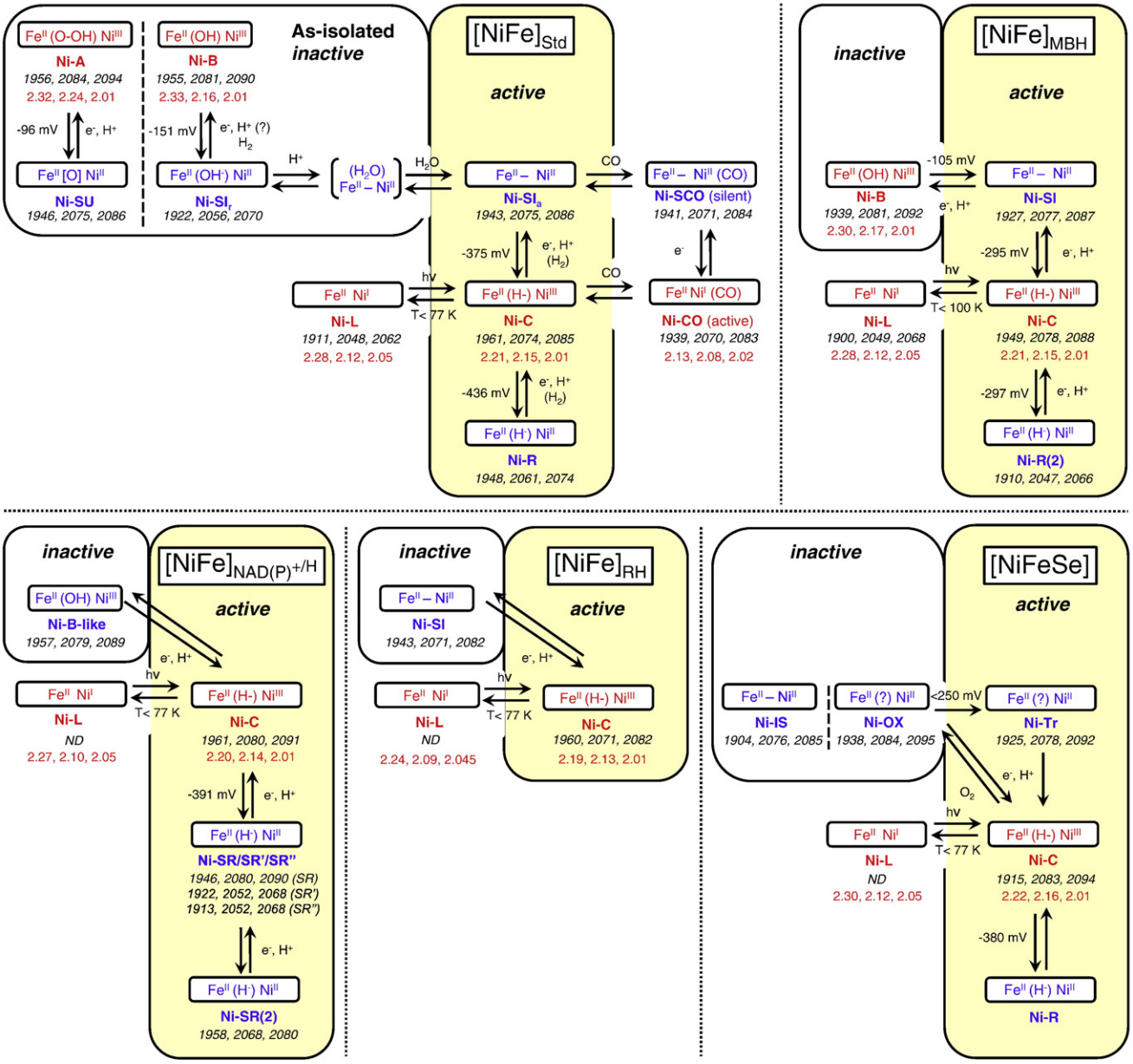

Fig. 2. Schematic overview of [NiFe] hydrogenase activation/deactivation, catalytic cycle, and light-sensitive states for standard and all nonstandard hydrogenases discussed in this review. Formal redox states for iron and nickel are indicated and bridging ligand identities are proposed in parentheses when known and brackets when speculative. EPR-active states with observed g-values are shown in red text; EPR-silent states are shown in blue. FTIR frequencies are given in cm^{-1} in black, italicized text. Redox potentials and FTIR frequencies of the standard [NiFe] hydrogenase are given for *Desulfovibrio vulgaris* Miyazaki F (*Dv*MF), taken from references [35–38]. EPR g-values for the standard [NiFe] hydrogenase are given for the *A. vinosum* hydrogenase, taken from reference [39]. Redox potentials, FTIR frequencies, and EPR g-values for the O_2-tolerant MBH are given for the *Aa* Hase I, taken from references [40–42]. FTIR frequencies and EPR g-values for the NAD(P)$^+$-reducing hydrogenase are given for the *Re* HoxHYFU protein complex [43] and the regulatory hydrogenase values are given for the *Re* protein [44]. For the [NiFeSe] protein, EPR g-values are given for the *Desulfovibrio baculatum* (*Db*) enzyme [45], and FTIR frequencies are given for the *Desulfovibrio vulgaris Hildenborough* (*Dv*H) enzyme [46].

Another common electrocatalytic trait of the O_2-tolerant MBHs is that H_2 oxidation requires an overpotential. Standard [NiFe] hydrogenases are very effective catalysts, with high catalytic activity initiated at essentially no overpotential [60]. On the other hand, hydrogen oxidation in all O_2-tolerant MBHs requires potentials significantly more positive than the $2H^+/H_2$ cell potential (50–100 mV, depending on the hydrogenase) [31,40,47,58]. While this is a small value compared to molecular hydrogen-producing catalysts [61], it represents a great amount of wasted energy on the part of the organism and would likely not persist against natural selection if it were extraneous; therefore, it is important to understand the functional role of this overpotential.

As shown in Fig. 2, standard hydrogenases have two mechanisms of inactivation. At high potential under anaerobic conditions, they form the ready, Ni-B state [62], which recovers rapidly when the potential is lowered. When inactivated by O_2, a mixture of Ni-B and a slowly-recovering (also known as unready) species, traditionally called Ni-A, is formed, along with some irreversible damage [63]. In the O_2-tolerant MBHs, only the rapidly reactivated state is formed. This observation is in good agreement with spectroscopic results, which indicate formation of only Ni-B in the oxidized state, as discussed further below. This Ni-B state reactivates *via* a single-electron reduction process at more positive potentials than the standard [NiFe] hydrogenases in a nearly reversible fashion. This positive reactivation potential

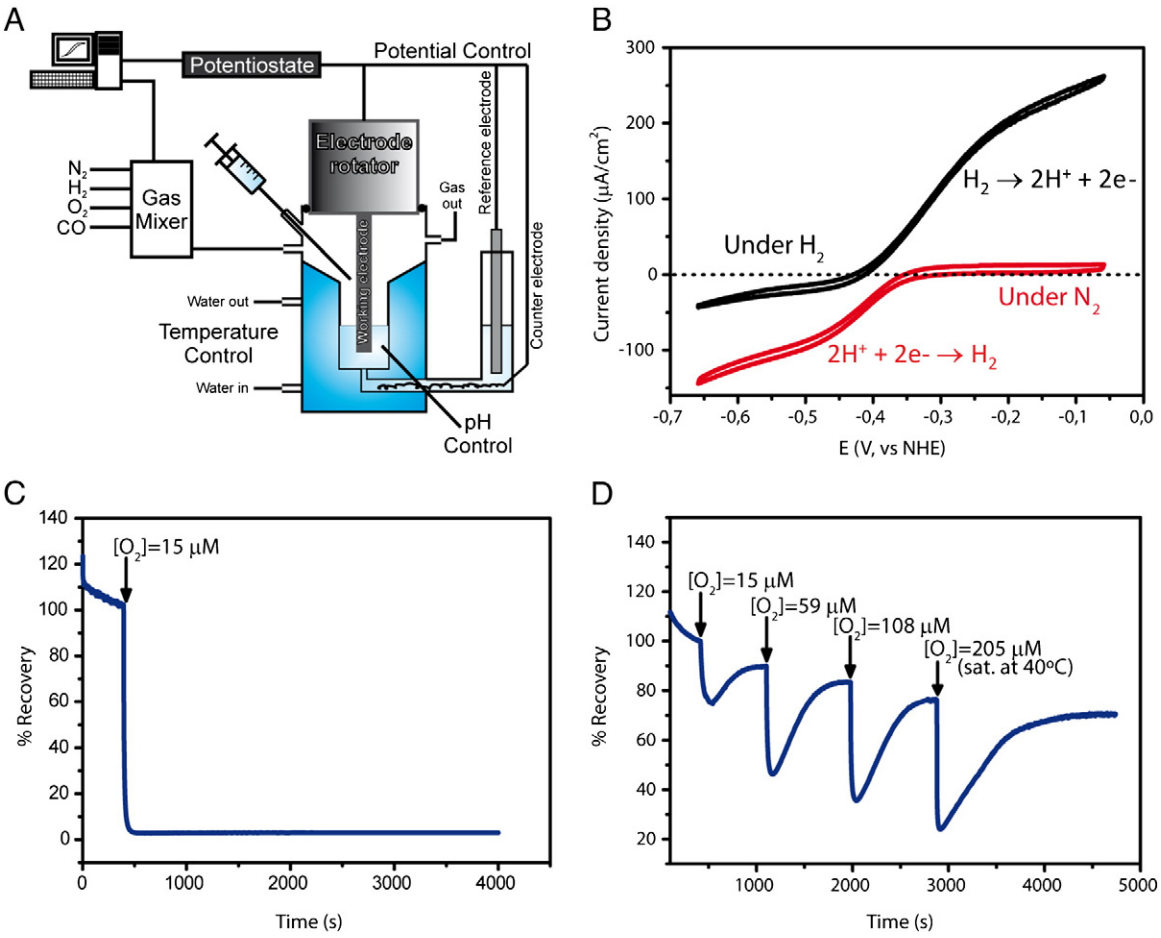

Fig. 3. (A) Electrochemical setup used for PFE experiments [52]. Protein is immobilized on a graphite electrode in a cell with a water jacket to control the temperature during the measurement. The electrode is rotated to avoid diffusion-limited kinetics. The electrochemical cell is continuously flushed with a gas mixture tuned by a set of mass flow controllers. (B) Cyclic voltammograms obtained for the [NiFe] hydrogenase from *Dv*MF covalently attached to a pyrolytic graphite electrode (PGE) as described in ref. [57]. Under a hydrogen environment (black curve), the enzyme catalyzes the oxidation of H_2 at almost no overpotential, but the H^+ reduction current is almost completely inhibited by the product. Under nitrogen, in the absence of H_2 (red curve), only the catalytic proton reduction current from the enzyme is observed. (C and D) Chronoamperometry experiments at +150 mV (*vs.* SHE) to measure hydrogen oxidation catalytic current of D*v*MF [NiFe] hydrogenase (C) and *Aa* Hase I immobilized on a PGE (D). Additions of aliquots of oxygen-saturated buffer are indicated. The cell is flushed continuously by a stream of hydrogen, at pH 7.0 and 40 °C (unpublished data from our laboratory).

is crucial to allow persistent H_2 oxidation in the presence of O_2 at physiologically accessible potentials [64,65]. The reversibility of this inactivation/reactivation process likely excludes the possibility of O_2 damage to the deeply buried iron sulfur clusters, for which reduction would not be fully reversible [66,67]. Similar characteristics have also been observed for *Ec* Hyd-1 and *Salmonella* O_2-tolerant MBHs, including positive reactivation potentials and existence of only one, rapidly reactivated, oxidation product [31,58].

The O_2-tolerant MBHs also display unique behavior with respect to CO binding. Carbon monoxide is known to be a strong inhibitor of standard hydrogenases and was shown to bind to nickel [18,68]. However, none of the studied O_2-tolerant MBHs showed significant inhibition of H_2 oxidation in the presence of CO, though the *Aa* protein did demonstrate weak interactions under high CO pressures [47,69] and CO inhibition for proton reduction was described for *Re* and *Rm* O_2-tolerant MBHs [59]. Because O_2 and CO are both hydrophobic gases of similar sizes, it is assumed that CO must also have access to the active site. The lack of inhibition thus suggests an inability of these O_2-tolerant MBHs to form a sufficiently strong Ni – CO bond to compete with hydrogen binding.

The inactivation and reactivation rates of the O_2-tolerant MBHs can also be compared to the standard hydrogenases. In both systems, oxygen inhibition is fast on the electrochemical timescale and increases with temperature, as expected for a diffusion-limited process, though when quantified it was found that the rates of reaction of *Re* HoxGK with O_2 are considerably lower than for the standard [NiFe] hydrogenases, for example, that of *Desulfovibrio gigas* [65,70]. This initially suggested that limited O_2 access to the active site may give rise to the oxygen tolerance of the enzyme. However, this is incompatible with the observation that oxygen tolerance of these MBHs also increases with temperature, implying that the rate of O_2 attack is not the controlling factor [71]. Furthermore, the rates of reactivation of the O_2-tolerant MBHs are more than two orders of magnitude faster than the standard [NiFe] hydrogenases and show a clear dependence on the potential of the electrode [40,47]. This important feature suggests that the capability for aerobic hydrogen oxidation is predominantly a characteristic extrinsic to the active site of the hydrogenase. This behavior provided some initial hints into understanding possible mechanisms behind oxygen tolerance in these hydrogenases.

The thermodynamics of gas selectivity were also studied by PFE. The H_2 concentration in the Knallgas bacteria habitat is approximately 10–180 ppm, while O_2 concentration is around 21% [72]. However, the *Re* HoxGK protein is capable of oxidizing H_2 at levels below 10 ppm H_2 in air [73]. This may suggest that high binding affinity towards H_2 ($K_M(H_2)$), in the presence of O_2 would keep the enzyme in the H_2 oxidation cycle. Indeed, $K_M(H_2)$ constants measured for *Re* and *Rm* O_2-tolerant MBHs were found to be lower than those measured for a majority of standard [NiFe] hydrogenases (6.1 μM and 0.57 μM,

respectively, at pH 5.5, 30 °C and −108 mV, for *Re* and *Rm*), similar to those found for *Ec* Hyd-1 under different experimental conditions [58,74]. But the fact that O_2 exposure rapidly results in decreased activity indicates that oxygen both reaches and reacts with the active site to form a redox state that requires reactivation [65]. Therefore, O_2 should not be viewed simply as a competitive inhibitor, but instead as a "competitive substrate" of H_2. Supporting this hypothesis, a study of the oxygen tolerance and $K_M(H_2)$ dependence on pH, temperature, and electrode potential revealed different trends for each property: Oxygen tolerance is increased at low electrode potentials and high temperatures but is not affected by pH; $K_M(H_2)$ increases with increasing electrode potential and temperature and is also independent of pH. At low potentials, oxygen-tolerant and oxygen-sensitive hydrogenases have similar $K_M(H_2)$ values and even show a similar "oxygen tolerance" [58]. On the other hand, in the O_2-tolerant MBHs, oxygen tolerance is increased at high temperatures, while $K_M(H_2)$ is decreased. This different behavior demonstrates that binding affinity towards H_2 is not a dominating factor in oxygen tolerance.

These numerous PFE studies suggested that the main factor conferring aerobic activity to these O_2-tolerant MBHs is not restricted O_2 diffusion to the active site, or an impediment of the active site towards reaction with O_2, but instead the ability of the hydrogenase to cope with O_2 once it reaches the active site. A mechanism for this was initially proposed some years ago [65], though spectroscopic and crystallographic investigations were required to gain a full understanding of these reactions on a molecular level.

2.2. The O_2-tolerant MBHs exhibit distinct spectroscopic signatures in the oxidized state

In addition to their shared electrocatalytic properties, the O_2-tolerant MBHs are generally thought to exhibit spectroscopic signatures that can be used for identification and classification. As mentioned above, the unready Ni-A state found in standard [NiFe] hydrogenases is absent in all O_2-tolerant MBHs; the oxidized protein exists only in the Ni-B state as observed by electron paramagnetic resonance (EPR) and Fourier ransform infrared (FTIR) spectroscopies. An initial hint about the nature of oxygen tolerance was provided by the observation that in this Ni-B state, there was extensive coupling between the oxidized nickel center and the iron sulfur clusters at low temperatures, giving complex features in the g ~ 2 region of the EPR spectrum [41,75]. This is shown in Fig. 4 for the *Aa* Hase I, and contrasts with the simple Ni-B spectrum of *Dv*MF that shows a single, oxidized [3Fe–4S] cluster with low g-anisotropy; these broad features are particularly pronounced at higher fields. Initial studies using pulsed EPR, ENDOR, and ESEEM techniques confirmed that the direct coordination environments around the nickel center were nearly identical for the oxidized *Re* HoxGK and the standard *Dv*MF proteins, though one hint provided by these experiments was that the additional HoxGK couplings could be simulated by including two distinct $S = 1/2$ species [76]. Potentiometric EPR titrations of *Aa* Hase I and *Ec* Hyd-1 revealed that all of the EPR signals could be accounted for by considering four, well-defined, single-electron transitions, albeit at a higher potential than the corresponding clusters in standard [NiFe] hydrogenases [41,77–79]. Under oxidizing conditions, the state accessed at the highest redox potentials couples strongly to both the [NiFe] center and the [3Fe–4S] center, so it was proposed to originate from the proximal iron sulfur cluster; mutation of the [3Fe–4S] cluster to an EPR-silent [4Fe–4S] cluster reduces the complex coupled EPR signals and confirms this assignment [79]. The new $S = 1/2$ signal was assigned to a high-potential (HP) transition in which the cluster reaches a superoxidized state [41]. This astonishing result introduced for the first time the idea that a single iron sulfur cluster could provide two reducing equivalents within the same protein [41].

The capability of this proximal [4Fe–4S] cluster to access three redox states under physiological potentials was suggested to originate from the presence of two additional, nearby cysteine residues, known as the supernumerary cysteines [30,41,80,81]. This was first proposed using homology modeling and comparison to native high-potential iron proteins and small-molecule models [41,82]. Spectroscopic techniques, including Mössbauer, EPR, and X-ray absorption, were used to glean information about the reactivity of this cluster prior to the availability of high-resolution crystal structures [41,83].

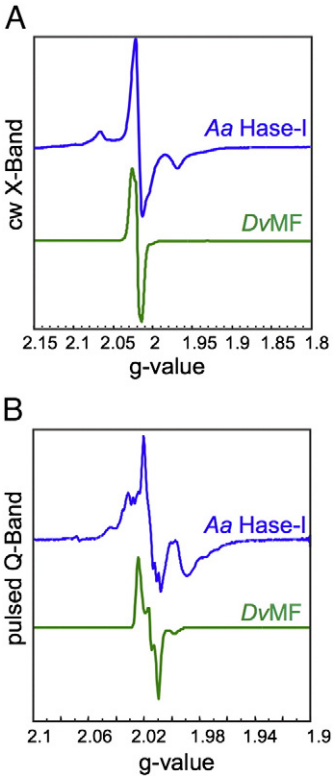

Fig. 4. (A) CW EPR spectra at X-band and (B) pseudo-modulated EPR spectra at Q-band, measured at 10 K, of as-isolated *Aa* Hase I and as-isolated [NiFe] hydrogenase from *DvMF* for comparison (for further details, see ref. [41]).

Recent spectroscopic studies probe the electronic structure of these unique clusters, complementing the structural data. Mössbauer studies of the superoxidized state of *Aa* Hase I identify one unique iron atom that can be attributed to the HP cluster. This iron exhibits a large isomer shift, consistent with an increased number of ligands and/or harder ligands, and a large quadrupole splitting, which reports on local geometric distortion [77]. Corresponding DFT calculations suggest that this iron is five-coordinate [77]. Additionally, EPR results from studies on *Ec* Hyd-1 reveal large hyperfine couplings to nitrogen nuclei in the HP state [79]. These spectroscopic signals can be interpreted in the context of the structural data to provide information on the dynamics of the cluster, which lies outside the capabilities of X-ray crystallography.

2.3. X-ray crystallography reveals a unique iron–sulfur cofactor structure

It is well established that determining the three-dimensional structure of a protein provides great insight into the mechanism of action of those proteins; this is obviously also true for hydrogenases [14,84]. Thus far, crystallographic studies have been performed to elucidate the detailed structure of both the standard [NiFe] hydrogenases and O_2-tolerant MBHs. In case of the standard hydrogenases, about 25 crystal structures have been reported for various redox states. Most of these structures were obtained from sulfate-reducing, anaerobic bacteria from the *Desulfovibrio* genus [10,23,68,85–87]. A membrane-associated, oxygen-sensitive hydrogenase from a photosynthetic bacterium, *Allochromatium vinosum*, has also been reported [88].

Very recently, crystal structures of the O_2-tolerant MBHs from *Re*, *Hydrogenovibrio marinus* (*Hm*) and *Ec* have been solved [81,89,90].

This represented a major breakthrough in understanding the mechanism of oxygen tolerance in these hydrogenases, for the structures showed very unique features for the proximal iron sulfur cluster, as discussed below. Aside from this, similar architectures with respect to the peptide fold and the metal centers, including the bimetallic active site and the other iron sulfur clusters, are found in both the standard hydrogenases and O_2-tolerant MBHs. The general structural motif of the hydrogen-uptake standard [NiFe] hydrogenase contains two subunits, one small (α, 35 kDa) and one large (β, 65 kDa), as shown in Fig. 1. In the small subunit of the MBHs, there is an extra C-terminus domain that is believed to anchor into the membrane for association with the aforementioned cytochrome.

In the small subunit, three Fe–S clusters are located in an almost linear fashion separated from the [NiFe] active site and each other by approximately 10 Å. As shown in Fig. 1, these Fe–S clusters generally consist of a "distal" [4Fe–4S] cluster coordinated by three cysteines and one histidine, a "medial" [3Fe–4S] cluster coordinated by three cysteines, and a "proximal" cluster. In standard hydrogenases, the proximal cluster is comprised of a standard [4Fe–4S] cubane coordinated by four cysteines [23,85]. In contrast, in the O_2-tolerant MBHs, this cluster has been shown to consist of an unusual [4Fe–3S] arrangement coordinated by six cysteines [81,89,90] and undergoes significant redox-dependent structural changes [89,90], as discussed below.

Two metal centers, the [NiFe] active site and a single Mg^{2+} center, are harbored in the large subunit. The Mg^{2+} ion is bound to a histidine residue at the C-terminus and participates in a hydrogen bond to the peptide backbone and a glutamate carboxylate side chain. This metal is commonly found in [NiFe] hydrogenases, though not in the subclass of [NiFeSe] hydrogenases, and may provide an anchor *via* the C-terminus histidine for the proton transfer pathway through the protein. This proposed proton transfer pathway is only slightly perturbed for the O_2-tolerant MBHs.

2.4. The [NiFe] active sites of the standard and O_2-tolerant MBHs are similar

In the middle of the large subunit, the [NiFe] active site is coordinated to the protein by four cysteine residues. Certain fundamental features are generally conserved among [NiFe] hydrogenases, independent of their oxygen tolerance. In the oxidized state, nickel is five-coordinate, with two terminal cysteine sulfur atoms, two bridging cysteine sulfur atoms, and a bridging ligand that varies depending on redox state. The bridging cysteines are also bound to iron. Additional non-proteinogenic ligands, two CN^- ligands and one CO ligand, are coordinated to iron [10,85]. The identity of these ligands was verified by FTIR spectroscopy [9]. The widely accepted model of the active site is shown in Fig. 1. To date, the crystal structures of three different oxidation states (aerobically isolated, chemically-(super) oxidized, and H_2-reduced) of the O_2-tolerant MBHs have been solved at atomic resolution [81,89,90]. In agreement with spectroscopic studies of the O_2-tolerant MBHs that have shown only one oxidized, Ni-B state, the crystal structure of the superoxidized state shows a hydroxo ligand bound in the bridging position [90,91]. After the two-electron reduction by hydrogen, the enzyme converts into the catalytically active state, where the bridging hydroxo ligand has been removed as water and a hydride is bound to this position instead [42,86,92]. The structures of the [NiFe] active site are almost identical to those found in the standard hydrogenases.

2.5. The most significant structural differences are found at the proximal iron sulfur cluster

As mentioned above, homology modeling and sequence alignment analysis of the small subunit had suggested that two extra cysteine residues exist close to the proximal iron sulfur cluster in the O_2-tolerant MBHs [41,80], giving this class of proteins the name "6C-hydrogenases". Specifically, a 'CXXCC' motif instead of 'CXXC' was recognized as an unusual sequence, while the electronic properties and high valency demonstrated by spectroscopic studies suggested distortion of this cluster. After solving the crystal structures, it became apparent that the proximal iron sulfur cluster has the unique structural features shown in Fig. 5. One of these extra cysteines is coordinated to the Fe atom, and the sulfur atom of the other extra cysteine forms part of the iron sulfur cluster instead of an inorganic sulfide, making this a formal [4Fe–3S] cluster. In the reduced (+3) state, the iron sulfur cluster forms a cubane shape though the replacement of this sulfur atom. However, in the super-oxidized state (+5), the cluster exists in two distinct and unusual conformations [90]. Both conformations show that one of the irons is displaced towards the cysteine residues and bound to the amide nitrogen of the extra cysteine. This coordination requires deprotonation of the amide, proposed to be carried out by the nearby glutamate residue, to form an unusual ligand-binding motif that had previously been observed in only two natural metalloproteins [93,94]. In the second conformation, the imide coordination persists, but an iron-thiolate bond is replaced by direct coordination to this glutamate. The presence of solution-phase conformers for *Ec* Hyd-1 was recently confirmed by an EPR study, which demonstrates two distinct sets of nitrogen couplings with different electronic properties. This report illustrates that the conformational distribution is not merely a crystallographic artifact [79], but instead may reflect a dynamical equilibrium between two states that interconvert with a relatively low barrier. In comparison, the Mössbauer studies of *Aa* Hase I suggest greater structural homogeneity, though it is possible that the electronic parameters of the unique iron are similar in both conformations, or the distribution between the two conformers changes in this protein, and signals from the second conformer exist within the resolution of the Mössbauer experiment (~20%) [77].

2.6. Genetic manipulation provides complementary information to electrochemical and spectroscopic results

Site-directed mutagenesis in conjunction with electrochemistry and spectroscopy has provided further insight into the nature of these supernumerary cysteines, which seem to be a necessary component of all O_2-tolerant MBHs discovered and may be ubiquitous throughout many species of microorganisms [30,32]. PFE studies on an *Re* HoxGK mutant show that substitution of both cysteines by glycines (Cys19Gly and Cys120Gly in *Re*, equivalent to Cys25 and

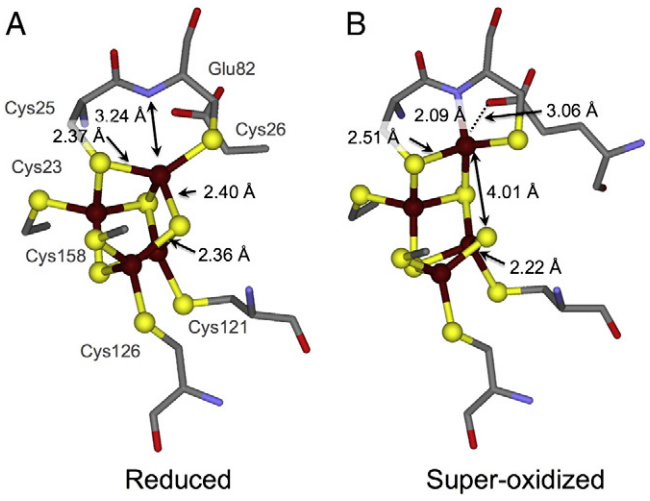

Fig. 5. Comparison of the *Hm* O_2-tolerant MBH proximal [4Fe–3S] cluster in the (A) H_2-reduced (PDB: 3AYX) and (B) super-oxidized (PDB: 3AYY) redox states. Cysteine residues directly coordinated to iron are labeled; bond lengths that differ by more than 0.1 Å between the two structures are indicated in the figure. For details, see ref. [89]. Only one of the conformations of the super-oxidized state is shown.

Cys126 in *Hm*) results in a protein that retains the high reactivation potentials and tolerates short pulses of O_2. Upon longer periods of O_2-exposure, however, catalytic activity was lost and could be recovered partially only after applying more negative potentials, indicating accumulation of species other than Ni-B [95]. For *Ec* Hyd-1, single and double mutants demonstrated that Cys19 was the critical cysteine for oxygen tolerance. The C19G and C19G/C120G mutants could not maintain H_2 oxidation during long exposures to O_2 while the C120G mutant behaved similarly to the wild type [96]. This is anticipated from the crystal structure of the cluster, which shows that the geometry of the iron coordinated to C19/C20 is the most perturbed upon oxidation [90]. Mutagenesis was also used for further EPR characterization of the iron-sulfur clusters in *Ec* Hyd-1. Conversion of the medial [3Fe–4S] cluster into a [4Fe–4S] cluster renders it magnetically-silent in the oxidized state, enabling the distinct EPR signals of the multiple HP conformations to be resolved and pulsed EPR experiments to parse out the $[4Fe–3S]^{5+}$ ligand sphere. Interestingly, in contrast to the distinct, $S = ½$ EPR spectrum of the *Aa* Hase I distal, reduced [4Fe–4S] cluster [41], the distal cluster of *Ec* Hyd-1 was not observed in EPR, which may suggest that the spin state is $S > ½$ [79]. Additional studies are required to fully elucidate the spin state of this cluster. This finding reflects the subtle role that the protein architecture can exert on local electronic properties and may directly relate to protein function.

2.7. Aerobic hydrogen oxidation activity in the O_2-tolerant MBHs requires rapid, successive electron transfers

Based on the spectroscopic, electrochemical, and crystallographic studies, a general mechanism behind the capability for aerobic activity in the O_2-tolerant MBH proteins has been proposed (Fig. 6). It is apparent that, in all O_2-tolerant MBHs, the unready Ni-A state is completely absent. For exclusive formation of the Ni-B state upon introduction of O_2, oxygen must be rapidly split into water and hydroxide in a four-electron, three-proton process. From spectroelectrochemical EPR titrations, it can be said that the first electron derives from the Ni(II)–Fe(II) active site, the conventional $[4Fe–3S]^{3+/4+}$ couple of the proximal cluster provides the second, the $[3Fe–4S]^{+/2+}$ couple of the medial cluster provides the third, and the fourth electron comes from the high-potential $[4Fe–3S]^{4+/5+}$ transition of the unique proximal cluster [30,41]. As mentioned above, the redox potentials of these clusters are higher than for their counterparts in the oxygen-sensitive, standard hydrogenases, as they must be tuned not just for the activation of hydrogen but also with respect to the reduction potentials of oxygen. It is generally stated that these electron transfers are "fast", though very little work has been done to address the kinetics of ET in hydrogenases. It is most likely that the electrons are transferred to oxygen *via* the active site one-by-one, and, though proton transfer is also necessary for water release, these steps are unlikely to be concerted [97]. The relative rates of each ET event are likely to vary significantly, as suggested in the standard [NiFe] hydrogenases [98]. The oxygen-binding event to the reduced [NiFe] site is almost necessarily concerted with a single-electron reduction from the bimetallic core to form a superoxide-like transient state. Therefore, in theory, this ET rate could be measured using the decrease of the reduced Ni-SI signal as a reporter. The second electron transferred reduces the superoxide moiety into a hydroperoxide species using the standard proximal $[4Fe–3S]^{3+/4+}$ couple, which should be fast because it requires little reorganization energy and is quite close to the active site [30]. The third electron comes from the reduced medial cluster and formally breaks the O – O bond into water and a hydroxyl radical. This is the most critical stage for the protein, because the hydroxyl radical is highly reactive and has a very high reduction potential, and it is likely that this is the step in which standard, oxygen-sensitive hydrogenases are trapped in the Ni-A state, having only three easily accessible electrons. In the O_2-tolerant MBHs, an extra electron from the proximal cluster is available to reduce the hydroxyl radical to hydroxide, the standard Ni-B bridging ligand. The crystal structures indicate that the HP transition requires large amounts of structural rearrangement (shown in Fig. 5), including elongation of an iron–sulfur bond by 1.6 Å and deprotonation of the backbone amide. From a Marcus-theory point of view, this increased reorganization energy should greatly impact the ET kinetics. However, the driving force of the electron transfer is also quite high, for the hydroxyl radical/water couple has a potential of 2.3 V at pH 7 [99], and ET rates are maximized when the reorganization energy matches the driving force. It was also shown

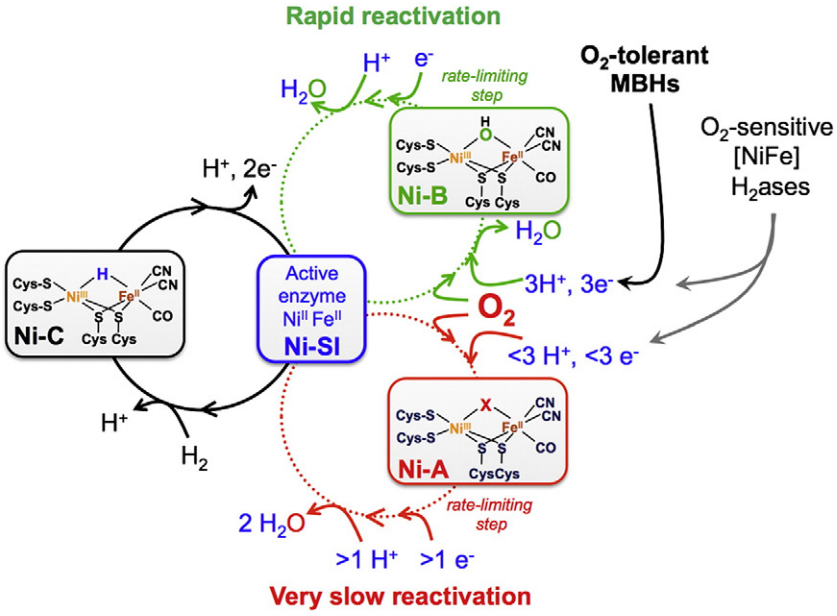

Fig. 6. Model showing the general scheme of the O_2-tolerant MBHs. Rapid H_2/H^+ cycling is the normal catalytic reaction of hydrogenase (black circle). In the presence of O_2, aerobic inactivation (thick arrow) of the O_2-tolerant MBH occurs, forming only the Ni-B state that can be rapidly reactivated (green circle) because the extra electron from the proximal cluster converts the O_2 molecule into the harmless hydroxide ligand. In standard, oxygen-sensitive [NiFe] hydrogenases, both the Ni-B state and the Ni-A state (red circle) are formed, requiring low potentials and long reactivation times to restore activity. The bridging ligand X in Ni-A has not been determined with confidence; proposed structures encompass an OOH- or OH-moiety.
Adapted from ref. [80] with modifications.

that the electronic coupling between the proximal cluster and the active site is an order of magnitude greater in the HP state than the reduced state, which will further enhance the kinetics of ET [77]. Thus, it can be imagined that these four electron transfer steps can occur sequentially yet very rapidly, possibly at near-activationless rates. This is critical for oxygen tolerance, because all electrons must be transferred into the active site before the partially-reduced transient species can form the Ni-A state. Once generated, the Ni-B state can be reactivated at high potentials to release water [58], thus enabling the protein to sustain hydrogen oxidation under aerobic conditions. This purported oxygen reductase, or "oxidase", activity is thus proposed as a general mechanism for reactivation of the protein, which is responsible for conferring oxygen tolerance to this class of proteins, as illustrated in Fig. 6.

Despite well-characterized spectroscopic signatures and crystal structures, there are still many questions about the O_2-tolerant MBHs that remain unanswered. It is still not understood why CO cannot bind strongly to the active site of most O_2-tolerant MBHs, as the active site possesses a very similar electronic structure to those of the standard hydrogenases [47,69]. These proteins show weaker hydride binding in the reduced Ni-C state than the standard [NiFe] hydrogenases [42,82], with the reduced states of *Ec* Hyd-1 showing only a Ni-L-like signal [79]. This observation provides the first experimental evidence that Ni-L, or an electronic state similar to Ni-L, may play an important catalytic role. Furthermore, as we attempted to describe above, the kinetics of these ET steps are potentially complicated and may be very interesting, for the actual rate of recovery should be governed by the ET and proton-coupled ET rates of the successive, single-electron reductions. The interplay between the iron–sulfur clusters—structures, spin-state and redox potentials—and catalytic activity may also prove to be a critical component, particularly for modulating ET kinetics. This is a pertinent topic to explore, particularly in the context of multi-electron transfer processes, which present a significant challenge for understanding (biological) small-molecule formation and activation.

3. Soluble oxygen-tolerant hydrogenases

3.1. NAD(P)$^+$-reducing hydrogenases form part of a large, multimeric protein system

The soluble, NAD(P)$^+$-reducing hydrogenase (HoxFUYH in *Re*) represents a different type of nonstandard hydrogenase found in aerobic microorganisms such as *Re*, *Rhodococcus opacus* (*Ro*), and *Alteromonas macleodii* (*Am*) [100–102], cyanobacteria such as *Synechocystis* (*Syn*) [103,104], and phototrophic bacteria such as *Thiocapsa roseopersicina* (*Tr*) [105]. These cytoplasmic protein systems are comprised of multi-subunit complexes that contain a heterodimeric hydrogenase moiety (HoxHY) along with a multimeric NAD(P)$^+$ diaphorase module (HoxFU) that reduces NAD^+ (or $NADP^+$) to NADH (or NADPH), as shown in Fig. 7; the inherent selectivity for NAD^+ over $NADP^+$ is currently unknown and may be species-dependent [8]. The NAD(P)$^+$-reducing hydrogenases primarily function as hydrogen-uptake proteins that transfer electrons directly from hydrogen to an associated flavin (FMN, FAD, or F_{420}) or NAD(P)$^+$ molecule within the diaphorase subunit; however, under reducing conditions, hydrogen production from NAD(P)H can also occur, causing these proteins to be referred to as "bidirectional" hydrogenases [106,107]. For the purposes of this review, the nomenclature and terminology of the *Re* protein, which represents one of the most studied NAD^+-reducing hydrogenases, will be used. In experiments to test the levels of oxygen tolerance in these enzymes, it was shown that the *Re* enzyme can oxidize hydrogen in the presence of air [108] while the isolated *Syn* enzyme is capable of reducing protons under oxygen [109]. Thus, these proteins are often designated "less oxygen-sensitive" than the standard hydrogenases. Another interesting aspect of these multimeric proteins (though beyond the scope of this review) is the analogy drawn between the NAD(P)$^+$-reducing subunits and the respiratory Complex I due to

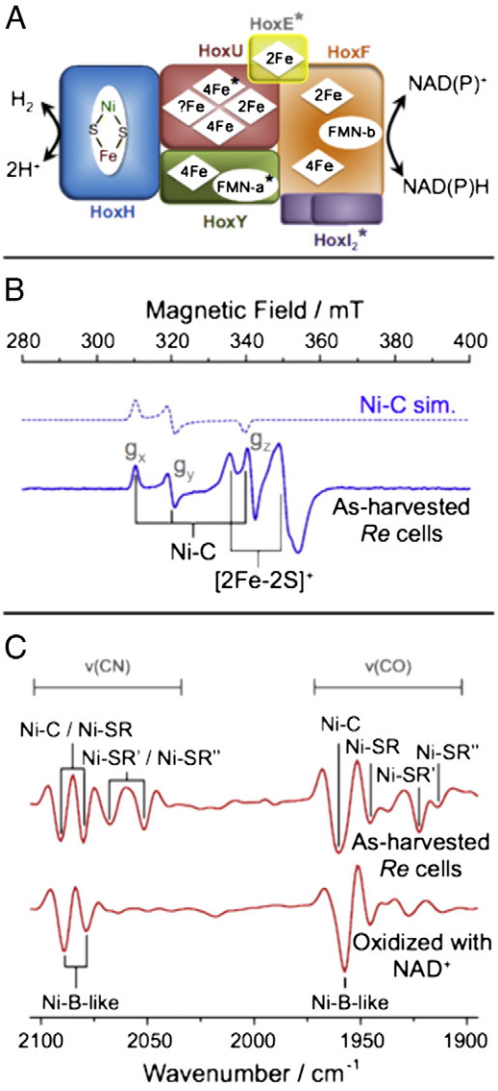

Fig. 7. (A) Schematic representation of the *Re* NAD(P)-linked bidirectional [NiFe] hydrogenase as a model; asterisks (*) indicate subunits or components not observed in all bidirectional hydrogenases from *Re*, *Ro*, *Tr*, and/or *Syn* [116]. "2Fe" and "4Fe" refer to [2Fe–2S] and [4Fe–4S] clusters, respectively. "?Fe" is most likely a [4Fe–4S] cluster, although a [3Fe–4S] cluster in certain bidirectional hydrogenases cannot be entirely excluded. (B) Results from *in situ* EPR studies on the soluble hydrogenase from *Re* in living cells; about 60% of the enzyme resides in the paramagnetic Ni-C state, which can be converted to more oxidized or reduced EPR-silent Ni(II) species. The signal from a $[2Fe–2S]^+$ cluster overlaps at g ~ 2. (C) The second derivative of the FTIR spectrum from the same sample exhibits a mixture of "standard-like" reduced states in the active site with a predominant contribution from Ni-C. Under oxidizing conditions, an almost pure (EPR-silent) "Ni-B-like" state of the enzyme is represented by one CO and two CN^- stretching bands in the second derivative of the IR spectrum, indicating a standard set of inorganic ligands at the active site.
Adapted from reference [111], with permission from Elsevier (copyright 2012).

function, sequence similarities, cofactor incorporation, and possible function in establishing a proton gradient across a membrane [110–112].

The hydrogenase subunit in *Re* consists of components HoxH, which contains the [NiFe] active site, and HoxY, which contains an iron sulfur cluster and FMN monomer [113]. Recent studies have reported the isolation of this heterodimeric protein, HoxHY, which represents the smallest, catalytically active sub-complex of the hydrogenase isolated thus far. Unlike the small subunit of standard and O_2-tolerant membrane-bound hydrogenases [84,85], the isolated HoxY unit is thought to contain only one proximal-type [4Fe–4S] cluster, with another [2Fe–2S] cluster likely in nearby proximity [114,115]. Over the years, investigating this class of proteins has presented many challenges. Though sequence analysis

suggests there should be many potential iron–sulfur binding domains [105,108,116], few EPR signals could be attributed to specific clusters or the active site in the oxidized state when the protein was studied *in vitro* [117,118]. The most prevalent signal to appear upon reduction of the protein was, in fact, a $[2Fe–2S]^+$ cluster, which is not found in any of the standard hydrogenases [117,118] Similarly, nickel-derived EPR signals that would report on the oxidation state of the active site were not observed to an appreciable extent in any accessible redox states [117,118]. The absence of well-defined EPR signals has since been attributed to magnetic coupling between paramagnetic species, possibly a Ni(III) center with [3Fe–4S] or [4Fe–4S] clusters, and complicates interpretation of metal-binding in the active enzyme. It may be that the close electronic and spin coupling between the subunits provides the necessary ET chain for efficient $NAD(P)^+$ reduction [111]. At this point, the iron–sulfur cluster ET chain in the $NAD(P)^+$-reducing hydrogenases remains poorly characterized.

3.2. Electrochemistry indicates bidirectional hydrogen cycling capability

In comparison to the O_2-tolerant hydrogenases, very few PFE studies have been done on the $NAD(P)^+$-reducing hydrogenases, probably due to the large size of these multimeric protein systems. Very recently, however, the isolated HoxHY module from *Re* was adsorbed on electrodes for electrochemical investigations [113]. In PFE, the as-isolated, oxidized enzyme is catalytically inactive and requires reductive activation at potentials close to the $2H^+/H_2$ reduction couple, which is close enough to the $NAD(P)^+$/NAD(P)H couple to suggest accessible *in vivo* activation. Once activated, no evidence of a reversible, anaerobic high-potential inactivation, as found in most hydrogenases, was detected. The enzyme showed catalytic activity for both H_2 oxidation and production, without requiring the overpotential observed in O_2-tolerant MBHs. At high potentials, the isolated enzyme reacts only slowly with oxygen to generate an inactive state that can be reactivated very fast at −384 mV, even in the presence of O_2. Additionally, another oxidized, inactive state that reactivates at more positive potentials was detected, though the nature and function of this state is unknown [113]. This suggests that *in vivo*, the low potential imposed by the coupling of HoxHY to the diaphorase module, and therefore to the NAD(P) + /NAD(P)H pool [119], might be sufficient to preserve H_2 oxidation activity in the presence of O_2; this redox-buffering could explain the observed aerobic activity of this enzyme. The NAD(P)-reducing hydrogenase from *Syn* was also investigated by PFE in the large, multimeric form. This hydrogenase showed features similar to the *Re* HoxHY, including bidirectionality, lack of an overpotential, two distinct states formed after O_2 inactivation which reactivated at different potentials, and H_2 production even in the presence of 1% O_2; this protein does not, however, demonstrate hydrogen oxidation in the presence of oxygen [109]. Hydrogen production and uptake assays on partially purified samples of the multimeric hydrogenases from *Tr* and *Am* indicate high stability in the presence of oxygen [105,120], and the latter enzyme retains 20% H–D exchange activity in the presence of 1% O_2, though PFE studies have not yet been performed [102]. The structural or enzymatic basis for this stability remains unknown because these biological characterization assays provide only limited information on these proteins.

3.3. Characterization of the active site of $NAD(P)^+$-reducing hydrogenases was facilitated by in vivo studies

The study of the $NAD(P)^+$-reducing hydrogenases using spectroscopic techniques has proven challenging for a number of reasons, including problems with generating pure protein preparations in high yields [105], identifying physiologically relevant states [118], and analyzing spectroscopic data [121–123]. Until recently [121,123,124], it was believed that the active site contained two additional cyanide ligands, including one to the nickel center, that conferred oxygen tolerance [121]. It had also been suggested that the bridging hydride and redox-active nickel center found in all [NiFe] hydrogenases were absent in this unique class. Initial spectroscopic studies on overexpressed, $NAD(P)^+$-reducing hydrogenase from *Syn* were the first to reveal that these proteins had a standard set of coordinating carbonyl and cyanide ligands, though evidence of a paramagnetic nickel center was absent from these EPR experiments [114]. Great advances towards understanding the catalytic mechanism of the $NAD(P)^+$-reducing hydrogenase were made in 2010, when EPR and FTIR studies were performed on the protein within whole *Re* cells [43]. These results demonstrated that the $NAD(P)^+$-reducing enzyme 1) contained a [NiFe] active site with the standard set of ligands (one carbonyl, two cyanides); 2) under *in vivo* conditions, 60% of the enzyme could be found in an EPR-active Ni-C state that exhibited cryogenic conversion to the Ni-L state, like the standard hydrogenases; and 3) required at least one $[2Fe–2S]^+$ cluster. FTIR studies also revealed the presence of multiple reduced, EPR-silent Ni-SR states; these critical results are highlighted in Fig. 7 [43].

3.4. The $NAD(P)^+$-reducing hydrogenases can be viewed as low potential oxygen-tolerant hydrogenases

As mentioned above, the $NAD(P)^+$-reducing hydrogenases exhibit some or all of the following traits: lack of an overpotential, hydrogen oxidation under aerobic conditions, and bidirectional proton reduction and hydrogen oxidation. However, the mechanism by which these proteins derive their purported oxygen tolerance remains unclear. Soluble $NAD(P)^+$-reducing hydrogenases do not have the special proximal cluster to provide extra electrons to the active site for rapid O_2 reduction, as found in the O_2-tolerant MBHs. Mutagenesis and genetic studies have provided some insight into which residues are critical for electron transfer, hydrogen activation, and oxygen tolerance [125,126]. In the *Re* HoxHY moiety isolated from the diaphorase subunits, hydrogen oxidation capability in the presence of oxygen was diminished, and it was found that potentials at or below those of the $NAD(P)^+$/NAD(P)H couple were required for reactivation of the protein [113]. All states were found to be EPR-silent, despite the presence of a [4Fe–4S] cluster that was revealed by XAS spectroscopy, and FTIR bands distinct from the whole-cell results were observed [110,113]. This suggests a critical role for the complex system of cofactors that couples the $2H^+/H_2$ reaction at the [NiFe] active site to the $NAD(P)^+$/NAD(P)H reduction. Intersubunit, protein–protein interactions may impact the potentials of the active site or iron sulfur clusters with respect to the ET chain within the diaphorase module; this may also tune the ET kinetics. A general hypothesis is that upon oxygen exposure, *in vivo*, the hydrogenase has ready access to electrons for the reduction of O_2 to H_2O and rapid reactivation. In this sense, H_2 and O_2 can be viewed as competitive substrates, as in the O_2-tolerant MBHs. This hypothesis is speculative, as there is no crystal structure of the hydrogenase and no rationale behind the slow, oxygen-independent inactivation. It is clear that many more studies are needed in order to fully understand how this class of hydrogenase can retain activity under aerobic or microaerobic conditions.

4. Regulatory hydrogenases (RHs)

Another class of soluble, nonstandard [NiFe] hydrogenase is the regulatory hydrogenase (RH). The most well-studied RH derives from *Re*; however, similar regulatory enzymes are found in photosynthetic bacteria such as *Rhodobacter capsulatus* (*Rc*) [127] and nitrogen-fixing bacteria such as *Bradyrhizobium japonicum* (*Bj*) [128]. These proteins contain an active site similar to the standard [NiFe] hydrogenases, exhibit high binding affinities for H_2, and are completely unaffected by oxygen. However, these oxygen-tolerant enzymes exhibit extremely low levels of activity, approximately 100-fold lower than the metabolic hydrogenases. Under reducing conditions or in the presence of hydrogen, the RH interacts as a

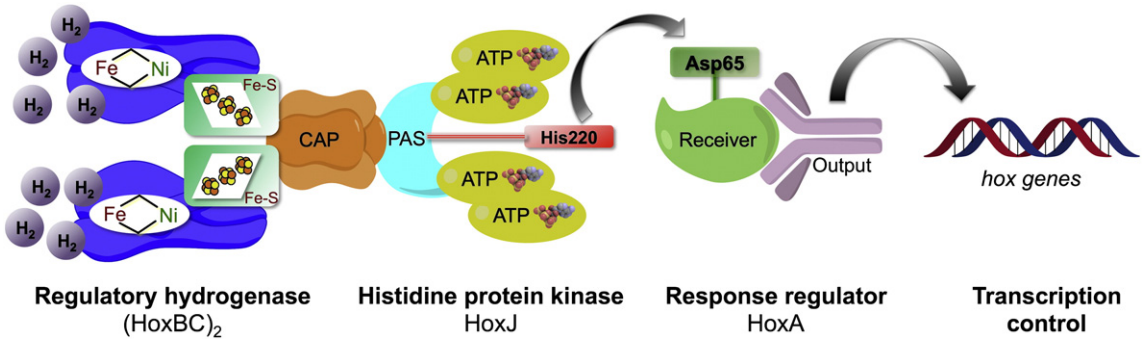

Fig. 8. Model scheme of the H_2-sensing RH from *Re* in its multimeric form and subsequent proteins involved in the signal transduction pathway for control of transcription. For further details, see ref. [108].

homodimer with a histidine protein kinase for downstream regulation of metabolic hydrogenase protein transcription, as shown in Fig. 8 [44].

4.1. Spectroscopic studies indicate a conserved active site with similar electronic properties

To the best of our knowledge, there have been no PFE studies on any RH, likely due to particularly low enzymatic activity. There are only two clearly identified redox states of the active site of the RH, as depicted in Fig. 2: an oxidized active site with FTIR frequencies resembling the Ni-SI state, and a reduced, hydride-bridged Ni-C state [44]. This state readily converts to the Ni-L state upon illumination, and requires several hours at high temperatures for complete regeneration of the Ni-C signal (>2 h at 200 K), suggesting either a sterically-hindered active site or particularly weak hydride binding [44]. FTIR studies confirm the presence of only two redox states and a standard ligand set on the iron [44]. The iron sulfur clusters of the small subunit of the RH also differ from those of the standard [NiFe] hydrogenases. Sequence analysis indicates that the RH has three [4Fe–4S] clusters, though upon reduction with hydrogen gas, the EPR spectrum showed only the nickel active site without a nearby paramagnetic iron sulfur center. Formation of Ni-C without a reduced proximal cluster proved advantageous for EPR spectroscopy, because pulsed EPR techniques could be applied to easily characterize the bridging ligand in the reduced state; these studies represented the first direct detection of a bridging hydride ligand in any protein [92].

Recent Mössbauer and EPR studies in our laboratory have been carried out for further characterization of both the active site and the iron sulfur clusters [129]. Mössbauer results provide the first definitive evidence that there are three [4Fe–4S] clusters in the RH, instead of the typical medial [3Fe–4S] cluster, along with a standard [NiFe] active site (Fig. 9). In the as-isolated state, all three [4Fe–4S] clusters are in the diamagnetic (+2) form. Two of the clusters are reduced with H_2, and addition of strong chemical reductants yields all three clusters in the paramagnetic (+1) state (Fig. 9). With pulsed EPR techniques, these reduced clusters could be characterized; at very low temperatures, splitting and line broadening was observed in the Ni-C EPR spectrum as well. This demonstrates coupling between the proximal cluster and the active site, though the interactions between the clusters are small. Another interesting result to come out of these studies was the characterization of the iron atom in the active site. Though remaining low-spin Fe(II) in all available redox states, the Mössbauer isomer shift and quadrupole splitting parameters changed considerably upon reduction to the Ni-C state, consistent with an increase in coordination number. This result confirms that in the as-isolated state, the bridging position between iron and nickel remains open, and it is occupied upon reduction, *i.e.*, with a hydride [92].

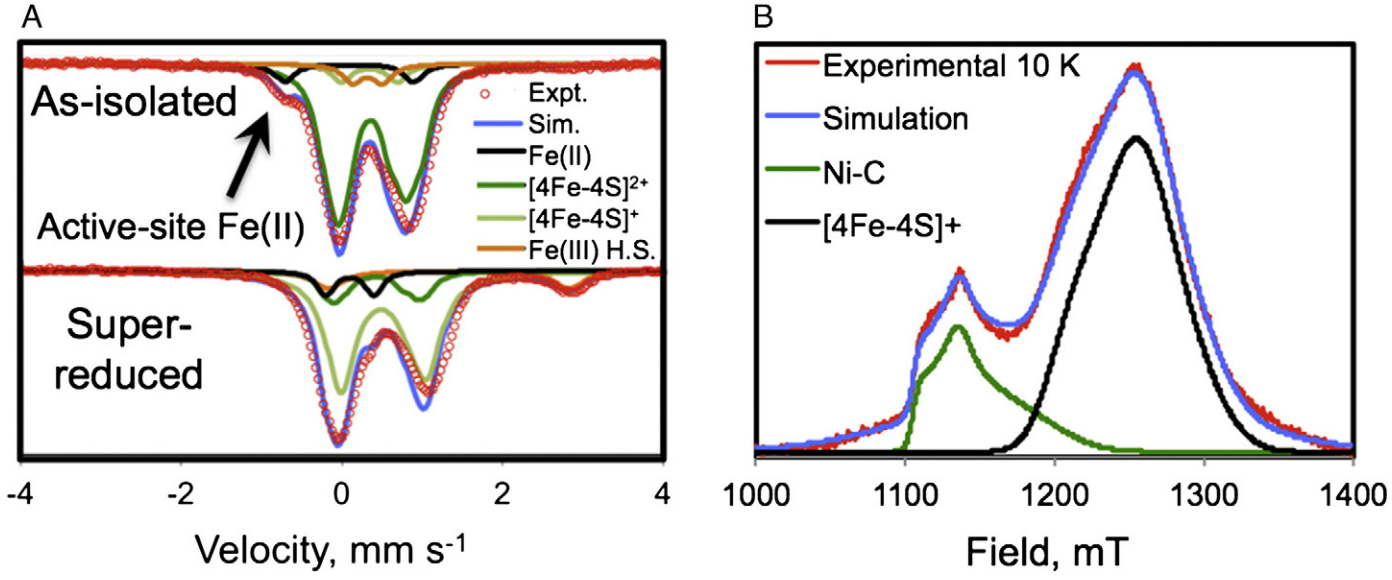

Fig. 9. (A) Mössbauer spectra of the as-isolated and the super-reduced forms of the RH of *Re* obtained at 80 K and 0 T. (B) Q-band field swept 2-pulse echo-detected EPR spectrum at 10 K of the sodium dithionite-reduced RH from *Re*. Signals from the [NiFe] active site and [4Fe–4S] clusters shown with simulations. Adapted from ref. [129].

4.2. Oxygen tolerance arises from a sterically constrained gas channel

Since there are only two stable redox states of the active site, and there is no X-ray structure of an RH, gaining information about the mechanism of activation and oxygen tolerance is challenging. Spectroscopic characterization by X-ray absorption spectroscopy indicated a change in the nickel coordination environment upon reduction, suggesting that the high affinity for hydrogen may be due to a pre-organized "transition state-like" conformation, though this is highly speculative [130]. Mutagenesis and homology modeling studies have provided the most information on the origin of oxygen tolerance. It was proposed that the oxygen tolerance of the RHs was provided by bulky amino acid residues creating an entrance channel for hydrophobic gases that is simply too small for anything larger than H_2 to enter. This hypothesis is consistent with the observed CO-tolerance of the enzymes [44], and when these isoleucine and phenylalanine side chains at the entrance of the purported hydrophobic gas channel are replaced for smaller amino acids, valine and leucine, hydrogen oxidation activity of the RH becomes sensitive to the presence of oxygen [127,131]. A similar approach has been applied to other hydrogenases, including the *Re* HoxGK, to probe whether introducing bulky side chains could confer some stability towards oxygen inactivation. These experiments were met with limited success; all mutants of the *Re* HoxGK exhibited both decreased hydrogen binding affinities and increased oxygen sensitivity [65,74,132,133]. Molecular dynamics studies were also used to examine the flexibility of the channel entrance under physiological conditions [134]. Interestingly, RH mutants that, when isolated, became sensitive to oxygen did not exhibit these same levels of oxygen sensitivity *in vivo*. These mutants were still able to bind the histidine kinase cofactor [127], indicating that the hydrogen oxidation and signaling events occur after the formation of the large complex between the RH homodimer and its kinase. The results from the RH mutants demonstrate the important role steric bulk can play in governing enzymatic activity, and suggest that protein engineering might be used successfully to confer oxygen tolerance to highly active enzymes.

5. Selenium-containing hydrogenases ([NiFeSe])

The final class of nonstandard [NiFe] hydrogenases to be addressed in this review includes those with a modified active-site cofactor. In a subgroup of the [NiFe] hydrogenases, one of the terminal cysteine thiolates on the nickel is replaced by a selenocysteine. This naturally-encoded amino acid has been identified as playing a critical role in an increasing number of proteins [135,136], particularly for anaerobic microorganisms [137], and [NiFeSe] hydrogenases are found in sulfate-reducing and methanogenic bacteria [138]. Selenocysteine is essentially isosteric to cysteine but exhibits different electronic properties, including greater polarizability and a decreased pK_a. Correspondingly, the [NiFeSe] hydrogenases are known to exhibit unique properties, including bias towards hydrogen production, high H/D exchange rates, increased overall activity, purported decreased oxygen sensitivity, and lack of EPR-active, oxidized states [136,139,140]. Additionally, in all [NiFeSe] proteins identified and similar to the RHs, the medial iron sulfur cluster is comprised of a [4Fe–4S] unit rather than the [3Fe–4S] unit observed in the standard [NiFe] hydrogenases [141–144]. However, as discussed further below, we note that caution should be exerted when using the term "oxygen-tolerant" to describe these proteins. In direct contrast to the O_2-tolerant MBHs, RHs, and some of the NAD(P)$^+$-reducing proteins, there has yet to be a [NiFeSe] hydrogenase identified that can oxidize hydrogen in the presence of oxygen. In these systems, hydrogen production can only be sustained in the presence of oxygen when low potentials are applied [145]. Despite this limitation, their favorable catalytic properties render them a subject of interest.

5.1. [NiFeSe] hydrogenases do not form the Ni-A or Ni-B state

The presence of selenium in certain hydrogenases was first demonstrated by X-ray absorption experiments at both the nickel and selenium absorption energies [146] and later confirmed by global incorporation of ^{77}Se for EPR experiments [147]. Though aerobic isolation of the protein results in an EPR-silent state, which led to the initial suggestion that these proteins might be oxygen tolerant [148], the H_2-reduced state of the [NiFeSe] hydrogenases shows a characteristic, light-sensitive Ni-C EPR signal that exhibits a large, anisotropic splitting when ^{77}Se is used due to approximately 10% spin delocalization onto the selenium atom [139,147]. Both the Ni-C and Ni-L EPR signals exhibit complex coupling to the reduced [4Fe–4S] clusters [45], though this has not yet been quantitatively addressed. As the oxidized state of the [NiFeSe] is EPR-silent, it can be inferred that, like the RHs and NAD(P)$^+$-reducing hydrogenases, these enzymes are incapable of forming the oxygen-inhibited Ni-B or Ni-A states; this also provides evidence of a [4Fe–4S] medial cluster, for an air-oxidized [3Fe–4S] cluster would be paramagnetic. FTIR and spectroelectrochemical studies of a [NiFeSe] protein from *Dv*H suggest that the aerobically-isolated protein exists in a state distinct from the high-potential or reoxidized state and requires reductive activation to enter the catalytic cycle [46]. The nature of this state has not been addressed, and thus far interpretation of these FTIR results has been complicated by the multiple isoforms that exist within a given protein preparation [46,144].

5.2. Structural characterization corroborates similarity to standard [NiFe] hydrogenases

Crystal structures of [NiFeSe] hydrogenases have been reported so far from *Db* and *Dv*H [141,144]. The overall protein fold resembles the standard [NiFe] hydrogenases as described in earlier sections, similar to crystallographic results from the O_2-tolerant MBHs. As mentioned above, the primary differences between [NiFeSe] and [NiFe] hydrogenase structures are found in the metal centers. In addition to a [4Fe–4S] medial cluster and selenocysteine coordination to the nickel (Fig. 1), an iron-binding site was observed at the C-terminus of the large subunit instead of a Mg^{2+} ion.

The first structure of a [NiFeSe] hydrogenase showed the protein in the reduced state, which revealed an open coordination site between nickel and iron (presumably containing a hydride ligand, which is invisible in crystallography) as in the standard hydrogenases [141]. Recently, the structure of the oxidized, as-isolated [NiFeSe] hydrogenase was reported from *Dv*H [144]. Unlike all previous crystal structures of oxidized hydrogenases, this structure lacked an oxygenic bridging ligand between the nickel and iron centers. Instead, the terminally bound cysteine was found to be modified to a cysteine-S-dioxide, in the first report of this metal coordination motif observed for a metalloprotein, though similar coordination environments have been reported in small-molecule complexes [144] and singly-oxidized cysteine ligands have been observed previously in structures of oxidized hydrogenases [84,87]. The terminal selenocysteine was also modified and was modeled to exist in three different conformations. Two of these conformations represent entirely new motifs for metal binding in hydrogenases. We note that the crystal structure should be interpreted with care, however, because the modeling is certainly made more complex by the presence of three distinct isoforms. As with the spectroscopic results, further crystallographic studies are required before this geometry can be firmly established as the relevant, active-site coordination in this class of hydrogenase. Irreversible oxygen damage to the active site during aerobic protein preparation can significantly impact the crystallographic interpretation [88], and it is important to ensure against any possible artifact.

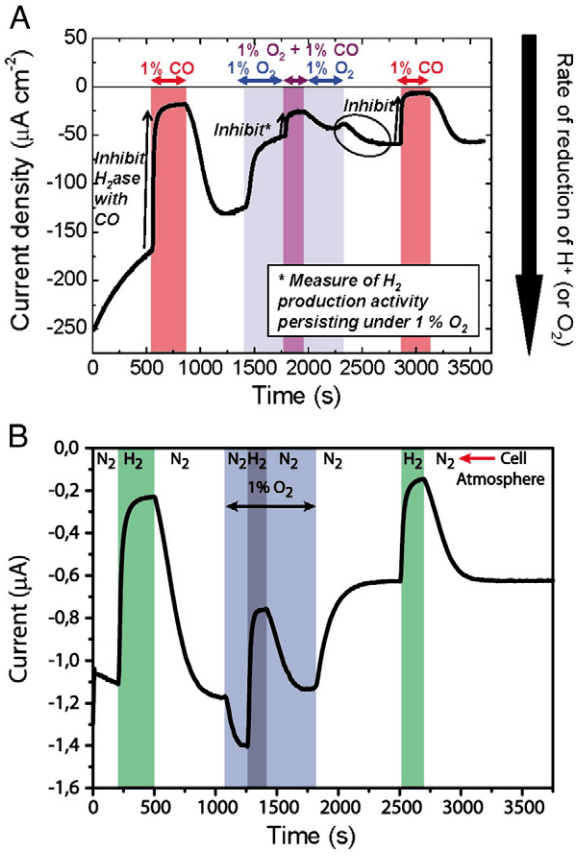

Fig. 10. (A) Probing the capacity for O_2 tolerance during H_2 production by *Db* [NiFeSe] hydrogenase. The enzyme was poised at −0.45 V (*vs.* NHE) under changing atmospheres of N_2, 1% CO in N_2, 1% O_2 in N_2 and 1% O_2 + 1%CO in N_2 as indicated in the plot. (B) Chronoamperometry experiment at −0.51 V (*vs.* NHE) to demonstrate that standard [NiFe] hydrogenases can also produce H_2 in the presence of 1% O_2. The electrode was covalently modified with *Dv*MF [NiFe] hydrogenase as described previously [57], and the gas mixture was varied during the experiment, similar to the procedure in A [109,145]. A, adapted with permission from ref. [145] (copyright 2008 American Chemical Society).

5.3. PFE studies of [NiFeSe] hydrogenases demonstrate hydrogen production in the presence of oxygen

To investigate catalytic activity, the [NiFeSe] hydrogenase from *Db* was adsorbed on PGE electrodes and studied by PFE. This enzyme shows high catalytic currents at low overpotential for both H_2 oxidation and H^+ reduction. Furthermore, proton reduction currents were detected even in the presence of H_2, which is usually a strong inhibitor of hydrogen production in standard [NiFe] hydrogenases (also called "product inhibition") [59]. Anaerobic inactivation of the enzyme does occur at high potentials, but in contrast with other hydrogenases, only under decreased H_2 concentration in the cell, suggesting that substrate binding protects the active site from high-potential inactivation. However, this hydrogenase does not maintain H_2 oxidation at high potentials in the presence of O_2; injection of small aliquots of oxygen-saturated buffer caused rapid, complete inactivation of the enzyme into two, catalytically distinct, inactive species. One of these aerobically-induced inactive states is preferentially generated under a hydrogen atmosphere and reactivates at the same, high potential as the anaerobically-inactivated state; in the absence of spectroscopic data, it has been assumed that these two methods give rise to the same inactive state. The second species is more interesting, as it reactivates quickly at a potential close to the $2H^+/H_2$ couple and is not detected after anaerobic inactivation. These factors hinted at the possibility of hydrogen production by hydrogenases in the presence of O_2, which was previously unknown behavior. In a complex chronoamperometry experiment combining the use of argon, CO and O_2, researchers were able to demonstrate that proton reduction currents from the [NiFeSe] hydrogenase persisted even when the cell was flushed with 1% O_2 (Fig. 10A). Therefore, it was claimed that this hydrogenase exhibits oxygen tolerance only for H_2 production, unlike the oxygen-tolerant MBHs and RHs [145].

Up to this point, H_2 production in the presence of O_2 was considered a feature limited to "oxygen-tolerant" hydrogenases, under the assumption that oxygen-sensitive hydrogenases were incapable of this behavior. While writing this review and motivated by the results found on the *Ec* Hyd-2 [58] and [NiFeSe] hydrogenases [145], which, despite being oxygen-sensitive for H_2 oxidation, showed H^+ reduction currents in the presence of O_2, we decided to perform a similar study to test this assumption. A chronoamperometry experiment on an electrode covalently modified with the standard, oxygen-sensitive [NiFe] hydrogenase from *Dv*MF (Fig. 10B) was carried out under varying gas atmospheres [57]. Initially, the proton reduction current was measured under 100% N_2. Changing the atmosphere to 100% H_2 demonstrates the anticipated product-induced inhibition. An 100% N_2 flow was used to flush out H_2 until a stable current was reached, after which 1% O_2 gas in N_2 was introduced to the cell. An increase in the measured current occurs due to direct O_2 reduction on the electrode. To discern if catalytic proton reduction current also remained, the bath gas was switched from N_2 to H_2. The current was observed to decrease, indicating inhibition of the enzyme and, equivalently, enzymatic activity that could be inhibited, even under 1% O_2. The gas was then switched back to 1% O_2 gas in N_2, and the increase in current indicates reactivation of the enzyme. Finally, O_2 was flushed out of the cell by N_2, and an inhibition step by H_2 was carried out to measure the final activity. We note that because [NiFeSe] hydrogenases do not show strong product inhibition by H_2, Parkin et al. had to use CO as an inhibitor [145], while we could use H_2 for the *Dv*MF protein. Thus, at low potentials, we conclude that this hydrogenase can also perform H_2 production in the presence of 1% O_2, similar to the behavior reported for *E. coli* Hyd-2, *Db* [NiFeSe] hydrogenase, or even the *Syn* NAD(P)$^+$-reducing hydrogenase [109]. This experiment demonstrates that when an electrode-immobilized enzyme is exposed to oxygen at negative potentials, the hydrogenase has access to sufficient electrons to reduce O_2 to water and form Ni-B, which rapidly reactivates and keeps the enzyme in the catalytic cycle for hydrogen production.

In the experiment shown in Fig. 10B, the enzyme is covalently bound to the electrode, which prevents protein film loss [57]. This difference precludes direct comparison to experiments in which the protein was simply adsorbed onto the electrode; however, it is apparent that the *Dv*MF [NiFe] hydrogenase does show some irreversible damage upon O_2 exposure because only approximately 50% of the initial current is recovered. In contrast, oxygen inhibition of the *Db* [NiFeSe] hydrogenase is nearly completely reversible; the decrease in current over time can be attributed strictly to film loss. Therefore, though proton reduction activity at negative potentials in the presence of oxygen is not an indicator of "oxygen tolerance", as demonstrated here, the [NiFeSe] protein does respond to long-term oxygen exposure differently than the standard oxygen-sensitive enzymes. The inability of the protein to form the unready Ni-A state may be the critical component for this difference.

5.4. Many possible factors contribute to the increased activity of [NiFeSe] hydrogenase

While a great deal of research in the 1990s was done to characterize the [NiFeSe] hydrogenases known at that time, very little information was gleaned that provided insight into its unique enzymatic activity. Interest has been renewed recently in light of potential biotechnological applications. Unfortunately, relatively few additional instructive studies have been performed so far. This may be due to challenges with protein purification and isolation; the *Dv*H [NiFeSe]

hydrogenase is membrane-bound, and, as discussed above, both spectroscopic and crystallographic studies revealed the presence of multiple isoforms within a presumably homogeneous preparation [144]. Theoretical methods have been used in an attempt to provide complementary information, though also with limited success [139]. DFT quantum chemical calculations on the active site reveal no significant differences in ligand binding, geometry, or orientation induced by the Se atom, and the spin distributions in the active states are nearly identical to those calculated for the standard [NiFe] hydrogenases [139]. Recent MD simulations indicate that the standard [NiFe] hydrogenase and [NiFeSe] hydrogenase sustain different H_2 partitioning coefficients within the enzyme [149], which may explain the decreased product inhibition on proton reduction activity [150]. From model compound work and supported by the recent crystal structure, it has also been suggested that, rather than binding to the bimetallic active site to form either the Ni-A or Ni-B state, oxygen exposure converts the selenocysteine into an oxidized selenate [144]. Because selenium–oxygen bonds are more labile than sulfur–oxygen bonds [45], the inactivated protein can be readily reactivated and thus exhibits little oxygen sensitivity [66,145]. The presence of a [4Fe–4S] medial cluster may also be relevant for understanding its catalytic activity. Relative to the standard [3Fe–4S] cluster, a [4Fe–4S] cluster is expected to have a lower redox potential, which may enhance electronic coupling between the active site and the protein surface; however, because related mutations on the standard [NiFe] hydrogenases to convert the [3Fe–4S] cluster into a [4Fe–4S] cluster had the effect of lowering the redox potential while leaving catalytic activity virtually unchanged, this appears unlikely [151]. Finally, the decreased pK_a of selenocysteine could also contribute to the enzymatic activity, particularly, the bias towards hydrogen production. Additional electrochemical, spectroscopic, and structural studies must be performed with highly homogeneous protein samples and well-documented control experiments to address these speculations.

6. Conclusions and future directions

6.1. Reconsidering the term "oxygen tolerance"

Oxygen tolerance has been considered the ability of a hydrogenase to maintain H_2 oxidation and/or H^+ reduction in the presence of O_2. The O_2-tolerant MBHs, RHs, and some of the NAD(P)$^+$-reducing proteins are capable of the former function, which is in accordance with the term "oxygen-tolerant". However, as demonstrated by our recent experiments, proton reduction on an electrode at negative potentials in the presence of oxygen is not sufficient to warrant designation as "oxygen-tolerant", for even oxygen-sensitive enzymes accomplish this. In most hydrogenases that can oxidize hydrogen aerobically, with the exception of the RHs, the reduced active site is known to interact with oxygen to give an oxygenic species in the bridging position. What differentiates these proteins from oxygen-sensitive enzymes is the exclusive formation of rapidly reactivated Ni-B or Ni-B-like states after O_2 exposure, instead of the inactive Ni-A state. As discussed earlier, this requires four electrons to be provided to oxygen in rapid succession, which recreates a localized, reduced cofactor environment [152]. We suggest that one distinction between these classes of nonstandard hydrogenases lies in the cofactor from which the extra electron(s) are accessed. The O_2-tolerant MBHs retrieve this electron from their proximal cluster, while the NAD(P)$^+$-reducing hydrogenases can retrieve electrons from stored NAD(P)H in their diaphorase subunit, as evidenced by their reactivation in the presence of NAD(P)H. As shown by mutagenesis studies, removal of these electron sources results in oxygen sensitivity. In contrast, it appears that the so-called "oxygen-tolerance" reported for the [NiFeSe] hydrogenases is not unique to the protein architecture. Instead, the previously observed electrocatalytic activity in the presence of O_2 likely arises from the close proximity of the electrode, which can supply electrons to the active site faster than deactivation can occur. It appears that the primary distinction between the [NiFeSe] hydrogenases and the standard hydrogenases is thus the absence of irreversible deactivation upon oxygen exposure. This may be correlated to the absence of an oxygenic bridge in the oxidized state, as revealed in the crystal structure. However, the hydrogen production activity of the [NiFeSe] protein in the presence of O_2 also relies on complete reduction of oxygen. Therefore, we propose that the nonstandard hydrogenases described here are simply more efficient oxygen reductases, or "oxidases," than their oxygen-sensitive counterparts, and as such suggest a revised protocol where these enzymes are classified on the basis of their oxidase activity rather than simply being designated "oxygen-tolerant".

6.2. Towards biotechnological application of hydrogenases

The study of hydrogenase proteins is motivated by two primary goals: understanding the complete catalytic mechanism in order to reproduce it in a synthetic chemical or protein-based system, and implementation of actual enzymes into biotechnological fuel cells. Due to their limited stability with respect to temperature, chemical interactions, and oxygen inactivation, the standard [NiFe] hydrogenases are not well suited for general-purpose application. Thus, more realistic prospects for implementation into devices lie with one of the "nonstandard" proteins. Here we have discussed the main classes of nonstandard [NiFe] hydrogenases to summarize their unique properties in the context of catalytic mechanism and inactivation/reactivation pathways.

Of these hydrogenases, we consider the O_2-tolerant MBHs to be the best understood and, at this point in time, have the greatest potential for practical application. In fact, a prototypical fuel cell based on the *Rm* O_2-tolerant MBH has already been demonstrated, showing that low levels of hydrogen in air can be used to power a small electrical load [153]. *Via* their membrane-associated C-terminus domain, the O_2-tolerant MBHs can be tethered to the membrane of a fuel cell or photovoltaic device or folded within reverse micelles and dissolved in organic solvents, which has also been carried out in prototypes [154–157]. Large-scale fermentative and/or phototrophic hydrogen generation is often discussed, particularly within policy venues, as model systems or organisms that contain hydrogenases directly coupled to photosystems I and II could be engineered for photoinduced hydrogen production [157–163]. Advantages of a cellular approach are evident in that biological systems exhibit certain characteristics that remain superior to those obtained in isolated proteins or synthetic models, including extremely high turnover numbers, low overpotential, and the capability of self-repair.

Gaining full understanding of the catalytic and activation/deactivation mechanisms of these hydrogenases is also necessary for the design of synthetic catalysts. Functional small-molecule models that reproduce components of the bimetallic core have already been shown [164–166], and tuning the secondary coordination sphere in these catalysts to simulate the protein environment has been effectively demonstrated [167]. Spectroscopic characterization of these models has also been used to provide insight into the protein systems [168,169]. A complementary approach may be the design or optimization of a *de novo*, hydrogen-producing enzyme. Protein and peptide engineering is a rapidly expanding field, with many synthetic and biochemical techniques readily accessible [19,170–173], and it is feasible to think that one could integrate the naturally optimized components of each class of hydrogenase within one protein. For example, the combination of the hydrogen-producing bias of the [NiFeSe] proteins with the supernumerary cysteines of the O_2-tolerant MBHs may yield a proton reduction catalyst with the inherent capability to rapidly reduce oxygen and therefore tolerate aerobic conditions, and incorporating elements such as a small gas channel and membrane insertion could further improve the system. To create this idealized protein, it is critical to first have a basic understanding of the complete mechanism and

identify the specific components of these enzymes that are responsible for the favorable characteristics. As this review highlights, these vital attributes are still largely unknown. A long-term objective such as this motivates the ongoing, fundamental research on these different hydrogenase proteins. By understanding how nature has devised distinct means for microorganisms to utilize a hydrogen-based metabolism in today's oxidizing atmosphere, we can begin to develop robust strategies towards an anthropogenic "hydrogen economy".

Acknowledgements

The authors would like to thank Dr. Eckhard Bill for helpful conversations, Birgit Deckers for assistance with the figures, and Drs. Federico Roncaroli and Maria Pandelia for sharing preprints of their manuscripts prior to publication. Financial support was provided by the Max Planck Society and an Alexander von Humboldt Foundation Postdoctoral Fellowship to H.S.S.

References

[1] World Energy Outlook, 2011.
[2] R. Cammack, M. Frey, R. Robson, Hydrogen as a Fuel: Learning from Nature, Taylor and Francis, London, 2001.
[3] R.F. Service, The hydrogen backlash, Science 305 (2004) 958–961.
[4] J. Rifkin, The Hydrogen Economy, Tarcher/Putnam, New York, 2002.
[5] R. Coontz, B. Hanson, Not so simple, Science 305 (2004) 957.
[6] J.A. Turner, Sustainable hydrogen production, Science 305 (2004) 972–974.
[7] P.M. Vignais, B. Billoud, J. Meyer, Classification and phylogeny of hydrogenases, FEMS Microbiol. Rev. 25 (2001) 455–501.
[8] P.M. Vignais, B. Billoud, Occurrence, classification, and biological function of hydrogenases: an overview, Chem. Rev. 107 (2007) 4206–4272.
[9] R.P. Happe, W. Roseboom, A.J. Pierik, S.P.J. Albracht, K.A. Bagley, Biological activation of hydrogen, Nature 385 (1997) 126–126.
[10] A. Volbeda, E. Garcin, C. Piras, A.L. De Lacey, V.M. Fernandez, C.E. Hatchikian, M. Frey, J.C. Fontecilla-Camps, Structure of the [NiFe] hydrogenase active site: evidence for biologically uncommon Fe ligands, J. Am. Chem. Soc. 118 (1996) 12989.
[11] A.J. Pierik, M. Hulstein, W.R. Hagen, S.P.J. Albracht, A low-spin iron with CN and CO as intrinsic ligands forms the core of the active site in [Fe]-hydrogenases, Eur. J. Biochem. 258 (1998) 572–578.
[12] M.L. Helm, M.P. Stewart, R.M. Bullock, M. Rakowski DuBois, D.L. DuBois, A synthetic nickel electrocatalyst with a turnover frequency above 100.000s^{-1} for H_2 production, Science 333 (2011) 863–866.
[13] S.E. Smith, J.Y. Yang, D.L. DuBois, R.M. Bullock, Reversible electrocatalytic production and oxidation of hydrogen at low overpotentials by a functional hydrogenase mimic, Angew. Chem. Int. Ed. 51 (2012) 3152–3155.
[14] A. Volbeda, J.C. Fontecilla-Camps, Structure–function relationships of nickel–iron sites in hydrogenase and a comparison with the active sites of other nickel–iron enzymes, Coord. Chem. Rev. 249 (2005) 1609–1619.
[15] X. Liu, S.K. Ibrahim, C.d. Tard, C.J. Pickett, Iron-only hydrogenase: synthetic, structural and reactivity studies of model compounds, Coord. Chem. Rev. 249 (2005) 1641–1652.
[16] S. Shima, O. Pilak, S. Vogt, M. Schick, M.S. Stagni, W. Meyer-Klaucke, E. Warkentin, R.K. Thauer, U. Ermler, The crystal structure of [Fe]-hydrogenase reveals the geometry of the active site, Science 321 (2008) 572–575.
[17] W. Lubitz, E. Reijerse, M. van Gastel, [NiFe] and [FeFe] hydrogenases studied by advanced magnetic resonance techniques, Chem. Rev. 107 (2007) 4331–4365.
[18] K.A. Vincent, A. Parkin, F.A. Armstrong, Investigating and exploiting the electrocatalytic properties of hydrogenases, Chem. Rev. 107 (2007) 4366–4413.
[19] W. Lubitz, E.J. Reijerse, J. Messinger, Solar water-splitting into H_2 and O_2: design principles of photosystem II and hydrogenases, Energy Environ. Sci. 1 (2008) 15–31.
[20] H. Ogata, W. Lubitz, Y. Higuchi, [NiFe] hydrogenases: structural and spectroscopic studies of the reaction mechanism, Dalton Trans. (2009) 7577–7587.
[21] M. Frey, Hydrogenases: hydrogen-activating enzymes, ChemBioChem 3 (2002) 153–160.
[22] S. Kamali, H. Wang, D. Mitra, H. Ogata, W. Lubitz, B.C. Manor, T.B. Rauchfuss, D. Byrne, V. Bonnefoy, F.E. Jenney, M.W.W. Adams, Y. Yoda, E. Alp, J. Zhao, S.P. Cramer, Observation of the FeCN and FeCO vibrations in the active site of [NiFe] hydrogenase by nuclear resonance vibrational spectroscopy, Angew. Chem. Int. Ed. 52 (2013) 724–728.
[23] Y. Higuchi, H. Ogata, K. Miki, N. Yasuoka, T. Yagi, Removal of the bridging ligand atom at the Ni Fe active site of [NiFe] hydrogenase upon reduction with H2, as revealed by X-ray structure analysis at 1.4 Å resolution, Structure 7 (1999) 549–556.
[24] A. Vanberkelarts, M. Dekker, C. Vandijk, H. Grande, W.R. Hagen, R. Hilhorst, M. Krusewolters, C. Laane, C. Veeger, Application of hydrogenase in biotechnological conversions, Biochimie 68 (1986) 201–209.
[25] H. Atomi, T. Sato, T. Kanai, Application of hyperthermophiles and their enzymes, Curr. Opin. Biotechnol. 22 (2011) 618–626.
[26] D.-H. Kim, M.-S. Kim, Hydrogenases for biological hydrogen production, Bioresour. Technol. 102 (2011) 8423–8431.
[27] C.M. English, C. Eckert, K. Brown, M. Seibert, P.W. King, Recombinant and *in vitro* expression systems for hydrogenases: new frontiers in basic and applied studies for biological and synthetic H_2 production, Dalton Trans. (2009) 9970–9978.
[28] M. Ludwig, T. Schubert, I. Zebger, N. Wisitruangsakul, M. Saggu, A. Strack, O. Lenz, P. Hildebrandt, B. Friedrich, Concerted action of two novel auxiliary proteins in assembly of the active site in a membrane-bound [NiFe] hydrogenase, J. Biol. Chem. 284 (2009) 2159–2168.
[29] M.R. Leach, D.B. Zamble, Metallocenter assembly of the hydrogenase enzymes, Curr. Opin. Chem. Biol. 11 (2007) 159–165.
[30] A. Parkin, F. Sargent, The hows and whys of aerobic H_2 metabolism, Curr. Opin. Chem. Biol. 16 (2012) 26–34.
[31] A. Parkin, L. Bowman, M.M. Roessler, R.A. Davies, T. Palmer, F.A. Armstrong, F. Sargent, How Salmonella oxidises H_2 under aerobic conditions, FEBS Lett. 586 (2012) 536–544.
[32] M.-E. Pandelia, W. Lubitz, W. Nitschke, Evolution and diversification of group 1 [NiFe] hydrogenases. Is there a phylogenetic marker for O_2-tolerance? Biochim. Biophys. Acta Bioenerg. 1817 (2012) 1565–1575.
[33] R.G. Sawers, S.P. Ballantine, D.H. Boxer, Differential expression of hydrogenase isoenzymes in *Escherichia coli* K-12: evidence for a third isoenzyme, J. Bacteriol. 164 (1985) 1324–1331.
[34] R.G. Sawers, D.J. Jamieson, C.F. Higgins, D.H. Boxer, Characterization and physiological roles of membrane-bound hydrogenase isoenzymes from *Salmonella typhimurium*, J. Bacteriol. 168 (1986) 398–404.
[35] C. Fichtner, C. Laurich, E. Bothe, W. Lubitz, Spectroelectrochemical characterization of the [NiFe] hydrogenase of *Desulfovibrio vulgaris* Miyazaki F, Biochemistry 45 (2006) 9706–9716.
[36] P. Kellers, M.-E. Pandelia, L.J. Currell, H. Goerner, W. Lubitz, FTIR study on the light sensitivity of the [NiFe] hydrogenase from *Desulfovibrio vulgaris* Miyazaki F: Ni-C to Ni-L photoconversion, kinetics of proton rebinding and H/D isotope effect, Phys. Chem. Chem. Phys. 11 (2009) 8680–8683.
[37] M.E. Pandelia, H. Ogata, L.J. Currell, M. Flores, W. Lubitz, Probing intermediates in the activation cycle of [NiFe] hydrogenase by infrared spectroscopy: the Ni-SIr state and its light sensitivity, J. Biol. Inorg. Chem. 14 (2009) 1227–1241.
[38] M.-E. Pandelia, H. Ogata, L.J. Currell, M. Flores, W. Lubitz, Inhibition of the [NiFe] hydrogenase from *Desulfovibrio vulgaris* Miyazaki F by carbon monoxide: an FTIR and EPR spectroscopic study, Biochim. Biophys. Acta Bioenerg. 1797 (2010) 304–313.
[39] B. Bleijlevens, B. Faber, S. Albracht, The [NiFe] hydrogenase from *Allochromatium vinosum* studied in EPR-detectable states: H/D exchange experiments that yield new information about the structure of the active site, J. Biol. Inorg. Chem. 6 (2001) 763–769.
[40] M.E. Pandelia, V. Fourmond, P. Tron-Infossi, E. Lojou, P. Bertrand, C. Leger, M.T. Giudici-Orticoni, W. Lubitz, Membrane-bound hydrogenase I from the hyperthermophilic bacterium *Aquifex aeolicus*: enzyme activation, redox intermediates and oxygen tolerance, J. Am. Chem. Soc. 132 (2010) 6991–7004.
[41] M.-E. Pandelia, W. Nitschke, P. Infossi, M.-T. Giudici-Orticoni, E. Bill, W. Lubitz, Characterization of a unique [FeS] cluster in the electron transfer chain of the oxygen tolerant [NiFe] hydrogenase from *Aquifex aeolicus*, Proc. Natl. Acad. Sci. U. S. A. 108 (2011) 6097–6102.
[42] M.-E. Pandelia, P. Infossi, M. Stein, M.-T. Giudici-Orticoni, W. Lubitz, Spectroscopic characterization of the key catalytic intermediate Ni-C in the O_2-tolerant [NiFe] hydrogenase I from *Aquifex aeolicus*: evidence of a weakly bound hydride, Chem. Commun. 48 (2012) 823–825.
[43] M. Horch, L. Lauterbach, M. Saggu, P. Hildebrandt, F. Lendzian, R. Bittl, O. Lenz, I. Zebger, Probing the active site of an O2-tolerant NAD(+)-reducing [NiFe]-hydrogenase from *Ralstonia eutropha* H16 by *in situ* EPR and FTIR spectroscopy, Angew. Chem. Int. Ed. 49 (2010) 8026–8029.
[44] M. Bernhard, T. Buhrke, B. Bleijlevens, A.L. De Lacey, V.M. Fernandez, S.P.J. Albracht, B.R. Friedrich, The H2 sensor of *Ralstonia eutropha*, J. Biol. Chem. 276 (2001) 15592–15597.
[45] M. Medina, E.C. Hatchikian, R. Cammack, Studies of light-induced nickel EPR signals in hydrogenase: comparison of enzymes with and without selenium, Biochim. Biophys. Acta Bioenerg. 1275 (1996) 227–236.
[46] A.L. De Lacey, C. Gutierrez-Sanchez, V.M. Fernandez, I. Pacheco, I.A.C. Pereira, FTIR spectroelectrochemical characterization of the Ni–Fe–Se hydrogenase from *Desulfovibrio vulgaris* Hildenborough, J. Biol. Inorg. Chem. 13 (2008) 1315–1320.
[47] K.A. Vincent, J.A. Cracknell, O. Lenz, I. Zebger, B. Friedrich, F.A. Armstrong, Electrocatalytic hydrogen oxidation by an enzyme at high carbon monoxide or oxygen levels, Proc. Natl. Acad. Sci. U. S. A. 102 (2005) 16951–16954.
[48] M. Bernhard, B. Benelli, A. Hochkoeppler, D. Zannoni, B. Friedrich, Functional and structural role of the cytochrome b subunit of the membrane-bound hydrogenase complex of *Alcaligenes eutrophus* H16, Eur. J. Biochem. 248 (1997) 179–186.
[49] S. Frielingsdorf, T. Schubert, A. Pohlmann, O. Lenz, B. Friedrich, A trimeric supercomplex of the oxygen-tolerant membrane-bound [NiFe]-hydrogenase from *Ralstonia eutropha* H16, Biochemistry 50 (2011) 10836–10843.
[50] M. Sezer, S. Frielingsdorf, D. Millo, N. Heidary, T. Utesch, M.-A. Mroginski, B. Friedrich, P. Hildebrandt, I. Zebger, I.M. Weidinger, Role of the HoxZ subunit in the electron transfer pathway of the membrane-bound [NiFe]-hydrogenase from *Ralstonia eutropha* immobilized on electrodes, J. Phys. Chem. B 115 (2011) 10368–10374.
[51] M. Brugna-Guiral, P. Tron, W. Nitschke, K.O. Stetter, B. Burlat, B. Guigliarelli, M. Bruschi, M.T. Giudici-Orticoni, [NiFe] hydrogenases from the hyperthermophilic bacterium *Aquifex aeolicus*: properties, function, and phylogenetics, Extremophiles 7 (2003) 145–157.

[52] F.A. Armstrong, N.A. Belsey, J.A. Cracknell, G. Goldet, A. Parkin, E. Reisner, K.A. Vincent, A.F. Wait, Dynamic electrochemical investigations of hydrogen oxidation and production by enzymes and implications for future technology, Chem. Soc. Rev. 38 (2009) 36–51.

[53] A.L. De Lacey, V.M. Fernandez, M. Rousset, R. Cammack, Activation and inactivation of hydrogenase function and the catalytic cycle: spectroelectrochemical studies, Chem. Rev. 107 (2007) 4304.

[54] Measurement of oxygen tolerance is impossible using redox mediators because low-potential acceptors would be re-oxidized by O_2, and high potential acceptors would inactivate the enzyme.

[55] O. Rüdiger, unpublished results, 2011.

[56] S.E. Lamle, S.P. Albracht, F.A. Armstrong, Electrochemical potential-step investigations of the aerobic interconversions of [NiFe]-hydrogenase from *Allochromatium vinosum*: Insights into the puzzling difference between unready and ready oxidized inactive states, J. Am. Chem. Soc. 126 (2004) 14899–14909.

[57] O. Rüdiger, J.M. Abad, E.C. Hatchikian, V.M. Fernandez, A.L. De Lacey, Oriented immobilization of *Desulfovibrio gigas* hydrogenase onto carbon electrodes by covalent bonds for nonmediated oxidation of H_2, J. Am. Chem. Soc. 127 (2005) 16008–16009.

[58] M.J. Lukey, A. Parkin, M.M. Roessler, B.J. Murphy, J. Harmer, T. Palmer, F. Sargent, F.A. Armstrong, How *Escherichia coli* is equipped to oxidize hydrogen under different redox conditions, J. Biol. Chem. 285 (2010) 3928.

[59] G. Goldet, A.F. Wait, J.A. Cracknell, K.A. Vincent, M. Ludwig, O. Lenz, B. Friedrich, F.A. Armstrong, Hydrogen production under aerobic conditions by membrane-bound hydrogenases from Ralstonia species, J. Am. Chem. Soc. 130 (2008) 11106–11113.

[60] Overpotential is defined here as the additional driving force required for activity with respect to the potential of the hydrogen couple under the specified measurement conditions.

[61] D.L. DuBois, R.M. Bullock, Molecular electrocatalysts for the oxidation of hydrogen and the production of hydrogen — the role of pendant amines as proton relays, Eur. J. Inorg. Chem. (2011) 1017–1027.

[62] D. Millo, P. Hildebrandt, M.-E. Pandelia, W. Lubitz, I. Zebger, SEIRA spectroscopy of the electrochemical activation of an immobilized NiFe hydrogenase under turnover and non-turnover conditions, Angew. Chem. Int. Ed. 50 (2011) 2632–2634.

[63] S.E. Lamle, S.P.J. Albracht, F.A. Armstrong, Electrochemical potential-step investigations of the aerobic interconversions of NiFe-hydrogenase from *Allochromatium vinosum*: insights into the puzzling difference between unready and ready oxidized inactive states, J. Am. Chem. Soc. 126 (2004) 14899–14909.

[64] D. Millo, M.-E. Pandelia, T. Utesch, N. Wisitruangsakul, M.A. Mroginski, W. Lubitz, P. Hildebrandt, I. Zebger, Spectroelectrochemical study of the NiFe hydrogenase from *Desulfovibrio vulgaris* Miyazaki F in solution and immobilized on biocompatible gold surfaces, J. Phys. Chem. B 113 (2009) 15344–15351.

[65] J.A. Cracknell, A.F. Wait, O. Lenz, B. Friedrich, F.A. Armstrong, A kinetic and thermodynamic understanding of O-2 tolerance in NiFe-hydrogenases, Proc. Natl. Acad. Sci. U. S. A. 106 (2009) 20681–20686.

[66] M.Y. Darensbourg, W. Weigand, Sulfoxygenation of active site models of [NiFe] and [FeFe] hydrogenases — a commentary on possible chemical models of hydrogenase enzyme oxygen sensitivity, Eur. J. Inorg. Chem. 2011 (2011) 994–1004.

[67] J.A. Imlay, Pathways of oxidative damage, Annu. Rev. Microbiol. 57 (2003) 395–418.

[68] H. Ogata, Y. Mizoguchi, N. Mizuno, K. Miki, S.-i. Adachi, N. Yasuoka, T. Yagi, O. Yamauchi, S. Hirota, Y. Higuchi, Structural studies of the carbon monoxide complex of [NiFe] hydrogenase from *Desulfovibrio vulgaris* Miyazaki: suggestion for the initial activation site for dihydrogen, J. Am. Chem. Soc. 124 (2002) 11628.

[69] M.E. Pandelia, P. Infossi, M.T. Giudici-Orticoni, W. Lubitz, The oxygen-tolerant hydrogenase I from *Aquifex aeolicus* weakly interacts with carbon monoxide: an electrochemical and time-resolved FTIR study, Biochemistry 49 (2010) 8873–8881.

[70] C. Leger, S. Dementin, P. Bertrand, M. Rousset, B. Guigliarelli, Inhibition and aerobic inactivation kinetics of desulfovibrio fructosovorans NiFe hydrogenase studied by protein film voltammetry, J. Am. Chem. Soc. 126 (2004) 12162.

[71] X. Luo, M. Brugna, P. Tron-Infossi, M.T. Giudici-Orticoni, E. Lojou, Immobilization of the hyperthermophilic hydrogenase from *Aquifex aeolicus* bacterium onto gold and carbon nanotube electrodes for efficient H-2 oxidation, J. Biol. Inorg. Chem. 14 (2009) 1275–1288.

[72] R. Conrad, Soil microorganisms as controllers of atmospheric trace gases (H-2, CO, CH4, OCS, N2O, and NO), Microbiol. Rev. 60 (1996) 609–640.

[73] J.A. Cracknell, K.A. Vincent, M. Ludwig, O. Lenz, B. Friedrich, F.A. Armstrong, Enzymatic oxidation of H-2 in atmospheric O-2: the electrochemistry of energy generation from trace H-2 by aerobic microorganisms, J. Am. Chem. Soc. 130 (2008) 424–425.

[74] M. Ludwig, J.A. Cracknell, K.A. Vincent, F.A. Armstrong, O. Lenz, Oxygen-tolerant H_2 oxidation by membrane-bound [NiFe] hydrogenases of Ralstonia species, J. Biol. Chem. 284 (2009) 465–477.

[75] O. Lenz, M. Ludwig, T. Schubert, I. Bürstel, S. Ganskow, T. Goris, A. Schwarze, B. Friedrich, H_2 conversion in the presence of O_2 as performed by the membrane-bound [NiFe]-hydrogenase of *Ralstonia eutropha*, ChemPhysChem 11 (2010) 1107–1119.

[76] M. Saggu, C. Teutloff, M. Ludwig, M. Brecht, M.-E. Pandelia, O. Lenz, B. Friedrich, W. Lubitz, P. Hildebrandt, F. Lendzian, R. Bittl, Comparison of the membrane-bound [NiFe] hydrogenases from *R. eutropha* H16 and *D. vulgaris* Miyazaki F in the oxidized ready state by pulsed EPR, Phys. Chem. Chem. Phys. 12 (2010) 2139–2148.

[77] M.-E. Pandelia, D. Bykov, R. Izsak, P. Infossi, M.-T. Giudici-Orticoni, E. Bill, F. Neese, W. Lubitz, Electronic structure of the unique [4Fe-3S] cluster in O_2-tolerant hydrogenases characterized by ^{57}Fe Mössbauer and EPR spectroscopy, Proc. Natl. Acad. Sci. U.S.A. 110 (2013) 483–488.

[78] M. Saggu, I. Zebger, M. Ludwig, O. Lenz, B. Friedrich, P. Hildebrandt, F. Lendzian, Spectroscopic insights into the oxygen-tolerant membrane-associated [NiFe] hydrogenase of *Ralstonia eutropha* H16, J. Biol. Chem. 284 (2009) 16264–16276.

[79] M.M. Roessler, R.M. Evans, R.A. Davies, J. Harmer, F.A. Armstrong, EPR spectroscopic studies of the Fe–S clusters in the O_2-tolerant [NiFe]-hydrogenase Hyd-1 from *Escherichia coli* and characterization of the unique [4Fe–3S] cluster by HYSCORE, J. Am. Chem. Soc. 134 (2012) 15581–15594.

[80] T. Goris, A.F. Wait, M. Saggu, J. Fritsch, N. Heidary, M. Stein, I. Zebger, F. Lendzian, F.A. Armstrong, B. Friedrich, O. Lenz, A unique iron–sulfur cluster is crucial for oxygen tolerance of a [NiFe]-hydrogenase, Nat. Chem. Biol. 7 (2011) 310–318.

[81] J. Fritsch, P. Scheerer, S. Frielingsdorf, S. Kroschinsky, B. Friedrich, O. Lenz, C.M.T. Spahn, The crystal structure of an oxygen-tolerant hydrogenase uncovers a novel iron–sulphur centre, Nature 479 (2011) 249–252.

[82] K. Knuttel, K. Schneider, A. Erkens, W. Plass, A. Muller, E. Bill, A.X. Trautwein, Redox properties of the metal centers in the membrane-bound hydrogenase from Alcaligenes-Eutrophus CH34, Bull. Pol. Acad. Sci. Chem. 42 (1994) 495–511.

[83] J. Fritsch, S. Loescher, O. Sanganas, E. Siebert, I. Zebger, M. Stein, M. Ludwig, A.L. De Lacey, H. Dau, B. Friedrich, O. Lenz, M. Haumann, [NiFe] and [FeS] cofactors in the membrane-bound hydrogenase of *Ralstonia eutropha* investigated by X-ray absorption spectroscopy: insights into O_2-tolerant H_2 cleavage, Biochemistry 50 (2011) 5858–5869.

[84] J.C. Fontecilla-Camps, A. Volbeda, C. Cavazza, Y. Nicolet, Structure/function relationships of [NiFe]- and [FeFe]-hydrogenases, Chem. Rev. 107 (2007) 4273–4303.

[85] A. Volbeda, M.H. Charon, C. Piras, E.C. Hatchikian, M. Frey, J.C. Fontecilla-Camps, Crystal structure of the nickel–iron hydrogenase from *Desulfovibrio gigas*, Nature 373 (1995) 580–587.

[86] S. Foerster, M. Stein, M. Brecht, H. Ogata, Y. Higuchi, W. Lubitz, Single crystal EPR studies of the reduced active site of [NiFe] hydrogenase from *Desulfiovibrio vulgaris* Miyazaki F, J. Am. Chem. Soc. 125 (2003) 83–93.

[87] H. Ogata, S. Hirota, A. Nakahara, H. Komori, N. Shibata, T. Kato, K. Kano, Y. Higuchi, Activation process of [NiFe] hydrogenase elucidated by high-resolution X-ray analyses: conversion of the ready to the unready state, Structure 13 (2005) 1635.

[88] H. Ogata, P. Kellers, W. Lubitz, The crystal structure of the [NiFe] hydrogenase from the photosynthetic bacterium *Allochromatium vinosum*: characterization of the oxidized enzyme (Ni-A state), J. Mol. Biol. 402 (2010) 428–444.

[89] Y. Shomura, K.-S. Yoon, H. Nishihara, Y. Higuchi, Structural basis for a [4Fe–3S] cluster in the oxygen-tolerant membrane-bound [NiFe]-hydrogenase, Nature 479 (2011) 253–256.

[90] A. Volbeda, P. Amara, C. Darnault, J.-M. Mouesca, A. Parkin, M.M. Roessler, F.A. Armstrong, J.C. Fontecilla-Camps, X-ray crystallographic and computational studies of the O_2-tolerant [NiFe]-hydrogenase 1 from *Escherichia coli*, Proc. Natl. Acad. Sci. U. S. A. 109 (2012) 5305–5310.

[91] M. van Gastel, C. Fichtner, F. Neese, W. Lubitz, EPR experiments to elucidate the structure of the ready and unready states of the [NiFe] hydrogenase of *Desulfolvibrio vulgaris* Miyazaki F, Biochem. Soc. Trans. 33 (2005) 7–11.

[92] M. Brecht, M. van Gastel, T. Buhrke, B. Friedrich, W. Lubitz, Direct detection of a hydrogen ligand in the [NiFe] center of the regulatory H-2-sensing hydrogenase from *Ralstonia eutropha* in its reduced state by HYSCORE and ENDOR spectroscopy, J. Am. Chem. Soc. 125 (2003) 13075–13083.

[93] W. Huang, J. Jia, J. Cummings, M. Nelson, G. Schneider, Y. Lindqvist, Crystal structure of nitrile hydratase reveals a novel iron centre in a novel fold, Structure 5 (1997) 691–699.

[94] J.W. Peters, M.H.B. Stowell, S.M. Soltis, M.G. Finnegan, M.K. Johnson, D.C. Rees, Redox-dependent structural changes in the nitrogenase P-cluster, Biochemistry 36 (1997) 1181–1187.

[95] J. Fritsch, O. Lenz, B. Friedrich, Structure, function and biosynthesis of O2-tolerant hydrogenases, Nat. Rev. Micro. 11 (2013) 106–114.

[96] M.J. Lukey, M.M. Roessler, A. Parkin, R.M. Evans, R.A. Davies, O. Lenz, B. Friedrich, F. Sargent, F.A. Armstrong, Oxygen-tolerant NiFe-hydrogenases: the individual and collective importance of supernumerary cysteines at the proximal Fe–S cluster, J. Am. Chem. Soc. 133 (2011) 16881–16892.

[97] J.J. Warren, T.A. Tronic, J.M. Mayer, Thermochemistry of proton-coupled electron transfer reagents and its implications, Chem. Rev. 110 (2010) 6961–7001.

[98] S. Dementin, B. Burlat, V. Fourmond, F. Leroux, P.P. Liebgott, A.A. Hamdan, C. Leger, M. Rousset, B. Guigliarelli, P. Bertrand, Rates of intra- and intermolecular electron transfers in hydrogenase deduced from steady-state activity measurements, J. Am. Chem. Soc. 133 (2011) 10211–10221.

[99] P.M. Wood, The potential diagram for oxygen at pH 7, Biochem. J. 253 (1988) 287–289.

[100] T. Burgdorf, E. van der Linden, M. Bernhard, Q.Y. Yin, J.W. Back, A.F. Hartog, A.O. Muijsers, C.G. de Koster, S.P.J. Albracht, B. Friedrich, The soluble NAD+-reducing [NiFe]-hydrogenase from *Ralstonia eutropha* H16 consists of six subunits and can be specifically activated by NADPH, J. Bacteriol. 187 (2005) 3122–3132.

[101] C. Grzeszik, M. Lubbers, M. Reh, H.G. Schlegel, Genes encoding the NAD-reducing hydrogenase of *Rhodococcus opacus* MR11, Microbiology 143 (1997) 1271–1286.

[102] W.A. Vargas, P.D. Weyman, Y. Tong, H.O. Smith, Q. Xu, [NiFe] hydrogenase from *Alteromonas macleodii* with unusual stability in the presence of oxygen and high temperature, Appl. Environ. Microbiol. 77 (2011) 1990–1998.

[103] K.K. Rao, D.O. Hall, Hydrogenases: isolation and assay, Methods Enzymol 167 (1988) 501–509.

[104] P. Tamagnini, R. Axelsson, P. Lindberg, F. Oxelfelt, R. Wanschiers, P. Lindblad, Hydrogenases and hydrogen metabolism of cyanobacteria, Microbiol. Mol. Biol. Rev. 66 (2002) 1–20.

[105] G. Rakhely, A.T. Kovacs, G. Maroti, B.D. Fodor, G. Csanadi, D. Latinovics, K.L. Kovacs, Cyanobacterial-type, heteropentameric, NAD(+)-reducing NiFe hydrogenase in

the purple sulfur photosynthetic bacterium *Thiocapsa roseopersicina*, Appl. Environ. Microbiol. 70 (2004) 722–728.
[106] J. Appel, S. Phunpruch, K. Steinmuller, R. Schulz, The bidirectional hydrogenase of Synechocystis sp. PCC 6803 works as an electron valve during photosynthesis, Arch. Microbiol. 173 (2000) 333–338.
[107] M. Kuhn, A. Steinbuchel, H.G. Schlegel, Hydrogen evolution by strictly aerobic hydrogen bacteria under anaerobic conditions, J. Bacteriol. 159 (1984) 633–639.
[108] T. Burgdorf, O. Lenz, T. Buhrke, E. van der Linden, A.K. Jones, S.P.J. Albracht, B. Friedrich, [NiFe]-hydrogenases of *Ralstonia eutropha* H16: modular enzymes for oxygen-tolerant biological hydrogen oxidation, J. Mol. Microbiol. Biotechnol. 10 (2005) 181–196.
[109] C.L. McIntosh, F. Germer, R. Schulz, J. Appel, A.K. Jones, The [NiFe]-hydrogenase of the cyanobacterium Synechocystis sp. PCC 6803 works bidirectionally with a bias to H_2 production, J. Am. Chem. Soc. 133 (2011) 11308–11319.
[110] L. Lauterbach, Z. Idris, K.A. Vincent, O. Lenz, Catalytic properties of the isolated diaphorase fragment of the NAD+-reducing [NiFe]-hydrogenase from *Ralstonia eutropha*, PLoS One 6 (2011) e25939.
[111] M. Horch, L. Lauterbach, O. Lenz, P. Hildebrandt, I. Zebger, NAD(H)-coupled hydrogen cycling — structure–function relationships of bidirectional [NiFe] hydrogenases, FEBS Lett. 586 (2012) 545–556.
[112] L.A. Sazanov, P. Hinchliffe, Structure of the hydrophilic domain of respiratory complex I from *Thermus thermophilus*, Science 311 (2006) 1430–1436.
[113] L. Lauterbach, J. Liu, M. Horch, P. Hummel, A. Schwarze, M. Haumann, K.A. Vincent, O. Lenz, I. Zebger, The hydrogenase subcomplex of the NAD(+)-reducing [NiFe] hydrogenase from *Ralstonia eutropha* — insights into catalysis and redox interconversions, Eur. J. Inorg. Chem. (2011) 1067–1079.
[114] F. Germer, I. Zebger, M. Saggu, F. Lendzian, R.D. Schultz, J. Appel, Overexpression, isolation, and spectroscopic characterization of the bidirectional [NiFe] hydrogenase from synechocystis sp. PCC 6803, J. Biol. Chem. 284 (2009) 36462–36472.
[115] K. Schneider, R. Cammack, H.G. Schlegel, Content and localization of FMN, Fe–S clusters and nickel in the NAD-linked hydrogenase of Nocardia-opaca 1b, Eur. J. Biochem. 142 (1984) 75–84.
[116] C. Eckert, M. Boehm, D. Carrieri, J. Yu, A. Dubini, P.J. Nixon, P.-C. Maness, Genetic analysis of the Hox hydrogenase in the Cyanobacterium Synechocystis sp. PCC 6803 reveals subunit roles in association, assembly, maturation, and function, J. Biol. Chem. 287 (2012) 43502–43515.
[117] R.P. Happe, W. Roseboom, G. Egert, C.G. Friedrich, C. Massanz, B. Friedrich, S.P.J. Albracht, Unusual FTIR and EPR properties of the H2-activating site of the cytoplasmic NAD-reducing hydrogenase from *Ralstonia eutropha*, FEBS Lett. 466 (2000) 259–263.
[118] E. van der Linden, T. Burgdorf, A.L. de Lacey, T. Buhrke, M. Scholte, V.M. Fernandez, B. Friedrich, S.P. Albracht, An improved purification procedure for the soluble [NiFe]-hydrogenase of *Ralstonia eutropha*: new insights into its (in) stability and spectroscopic properties, J. Biol. Inorg. Chem. 11 (2006) 247–260.
[119] H.A. Reeve, L. Lauterbach, P.A. Ash, O. Lenz, K.A. Vincent, A modular system for regeneration of NAD cofactors using graphite particles modified with hydrogenase and diaphorase moieties, Chem. Comm. 48 (2012) 1589–1591.
[120] G. Rakhely, T.V. Laurinavichene, A.A. Tsygankov, K.L. Kovacs, The role of Hox hydrogenase in the H-2 metabolism of *Thiocapsa roseopersicina*, Biochim. Biophys. Acta Bioenerg. 1767 (2007) 671–676.
[121] B. Bleijlevens, T. Buhrke, E. van der Linden, B. Friedrich, S.P.J. Albracht, The auxiliary protein HypX provides oxygen tolerance to the soluble [NiFe]-hydrogenase of *Ralstonia eutropha* H16 by way of a cyanide ligand to nickel, J. Biol. Chem. 279 (2004) 46686–46691.
[122] T. Burgdorf, S. Löscher, P. Liebisch, E. Van der Linden, M. Galander, F. Lendzian, W. Meyer-Klaucke, S.P.J. Albracht, B. Friedrich, H. Dau, M. Haumann, Structural and oxidation-state changes at its nonstandard Ni–Fe site during activation of the NAD-reducing hydrogenase from *Ralstonia eutropha* detected by X-ray absorption, EPR, and FTIR spectroscopy, J. Am. Chem. Soc. 127 (2005) 576–592.
[123] Z. Gu, J. Dong, C.B. Allan, S.B. Choudhury, R. Franco, J.J.G. Moura, I. Moura, J. LeGall, A.E. Przybyla, W. Roseboom, S.P.J. Albracht, M.J. Axley, R.A. Scott, M.J. Maroney, Structure of the Ni sites in hydrogenases by X-ray absorption spectroscopy. Species variation and the effects of redox poise, J. Am. Chem. Soc. 118 (1996) 11155–11165.
[124] S. Löscher, T. Burgdorf, I. Zebger, P. Hildebrandt, H. Dau, B. Friedrich, M. Haumann, Bias from H_2 cleavage to production and coordination changes at the Ni–Fe active site in the NAD+-reducing hydrogenase from *Ralstonia eutropha*, Biochemistry 45 (2006) 11658–11665.
[125] C. Massanz, B. Friedrich, Amino acid replacements at the H_2-activating site of the NAD-reducing hydrogenase from *Alcaligenes eutrophus*, Biochemistry 38 (1999) 14330–14337.
[126] T. Burgdorf, A.L. De Lacey, B. Friedrich, Functional analysis by site-directed mutagenesis of the NAD(+)-reducing hydrogenase from *Ralstonia eutropha*, J. Bacteriol. 184 (2002) 6280–6288.
[127] O. Duché, S. Elsen, L. Cournac, A. Colbeau, Enlarging the gas access channel to the active site renders the regulatory hydrogenase HupUV of *Rhodobacter capsulatus* O2 sensitive without affecting its transductory activity, FEBS J. 272 (2005) 3899–3908.
[128] L.K. Black, C. Fu, R.J. Maier, Sequences and characterization of hupU and hupV genes of *Bradyrhizobium japonicum* encoding a possible nickel-sensing complex involved in hydrogenase expression, J. Bacteriol. 176 (1994) 7102–7106.
[129] F. Roncaroli, M.-E. Pandelia, E. Bill, B. Friedrich, O. Lenz, W. Lubitz, The regulatory [NiFe] hydrogenase from *Ralstonia eutropha* studied by Mössbauer and pulse EPR spectroscopy, in preparation.
[130] M. Haumann, A. Porthun, T. Buhrke, P. Liebisch, W. Meyer-Klaucke, B. Friedrich, H. Dau, Hydrogen-induced structural changes at the nickel site of the regulatory [NiFe] hydrogenase from *Ralstonia eutropha* detected by X-ray absorption spectroscopy, Biochemistry 42 (2003) 11004–11015.
[131] T. Buhrke, O. Lenz, N. Krauss, B. Friedrich, Oxygen tolerance of the H_2-sensing [NiFe] hydrogenase from *Ralstonia eutropha* H16 is based on limited access of oxygen to the active site, J. Biol. Chem. 280 (2005) 23791–23796.
[132] F. Leroux, P.P. Liebgott, L. Cournac, P. Richaud, A. Kpebe, B. Burlat, B. Guigliarelli, P. Bertrand, C. Leger, M. Rousset, S. Dementin, Is engineering O-2-tolerant hydrogenases just a matter of reproducing the active sites of the naturally occurring O-2-resistant enzymes? Int. J. Hydrogen Energy 35 (2010) 10770–10777.
[133] P.-P. Liebgott, A.L. de Lacey, B. Burlat, L. Cournac, P. Richaud, M. Brugna, V.M. Fernandez, B. Guigliarelli, M. Rousset, C. Léger, S. Dementin, Original design of an oxygen-tolerant [NiFe] hydrogenase: major effect of a valine-to-cysteine mutation near the active site, J. Am. Chem. Soc. 133 (2011) 986.
[134] V.H. Teixeira, A.M. Baptista, C.M. Soares, Pathways of H2 toward the active site of [NiFe]-hydrogenase, Biophys. J. 91 (2006) 2035–2045.
[135] T.C. Stadtman, Selenocysteine, Annu. Rev. Biochem. 65 (1996) 83–100.
[136] M. Birringer, S. Pilawa, L. Flohe, Trends in selenium biochemistry, Nat. Prod. Rep. 19 (2002) 693–718.
[137] Y. Zhang, H. Romero, G. Salinas, V.N. Gladyshev, Dynamic evolution of selenocysteine utilization in bacteria: a balance between selenoprotein loss and evolution of selenocysteine from redox active cysteine residues, Genome Biol. 7 (2006).
[138] C.S.A. Baltazar, M.C. Marques, C.M. Soares, A.M. DeLacey, I.A.C. Pereira, P.M. Matias, Nickel–iron–selenium hydrogenases — an overview, Eur. J. Inorg. Chem. (2011) 948–962.
[139] M. Stein, W. Lubitz, The electronic structure of the catalytic intermediate Ni-C in [NiFe] and [NiFeSe] hydrogenases, Phys. Chem. Chem. Phys. 3 (2001) 5115–5120.
[140] C. Aldag, I.A. Gromov, I. Garcia-Rubio, K. von Koenig, I. Schlichting, B. Jaun, D. Hilvert, Probing the role of the proximal heme ligand in cytochrome P450cam by recombinant incorporation of selenocysteine, Proc. Natl. Acad. Sci. 106 (2009) 5481–5486.
[141] E. Garcin, X. Vernede, E.C. Hatchikian, A. Volbeda, M. Frey, J.C. Fontecilla-Camps, The crystal structure of a reduced [NiFeSe] hydrogenase provides an image of the activated catalytic center, Structure 7 (1999) 557–566.
[142] F.M.A. Valente, P.M. Pereira, S.S. Venceslau, M. Regalla, A.V. Coelho, I.A.C. Pereira, The [NiFeSe] hydrogenase from *Desulfovibrio vulgaris* Hildenborough is a bacterial lipoprotein lacking a typical lipoprotein signal peptide, FEBS Lett. 581 (2007) 3341–3344.
[143] M. Marques, R. Coelho, I.A.C. Pereira, P.M. Matias, Purification, crystallization and preliminary crystallographic analysis of the [NiFeSe] hydrogenase from *Desulfovibrio vulgaris* Hildenborough, Acta Crystallogr Sect F Struct Biol Cryst Commun. 65 (2009) 920–922.
[144] M.C. Marques, R. Coelho, A.L. De Lacey, I.A.C. Pereira, P.M. Matias, The three-dimensional structure of [NiFeSe] hydrogenase from *Desulfovibrio vulgaris* Hildenborough: a hydrogenase without a bridging ligand in the active site in its oxidised, "as-isolated" state, J. Mol. Biol. 396 (2010) 893–907.
[145] A. Parkin, G. Goldet, C. Cavazza, J.C. Fontecilla-Camps, F.A. Armstrong, The difference a Se makes? Oxygen-tolerant hydrogen production by the [NiFeSe]-hydrogenase from *Desulfomicrobium baculatum*, J. Am. Chem. Soc. 130 (2008) 13410–13416.
[146] M.K. Eidsness, R.A. Scott, B.C. Prickril, D.V. DerVartanian, J. Legall, I. Moura, J.J. Moura, H.D. Peck, Evidence for selenocysteine coordination to the active site nickel in the [NiFeSe]hydrogenases from *Desulfovibrio baculatus*, Proc. Natl. Acad. Sci. 86 (1989) 147–151.
[147] O. Sorgenfrei, A. Klein, S.P.J. Albracht, Influence of illumination on the electronic interaction between Se-77 and nickel in active F420-non-reducing hydrogenase from Methanococcus-Voltae, FEBS Lett. 332 (1993) 291–297.
[148] F.M.A. Valente, A.S.F. Oliveira, N. Gnadt, I. Pacheco, A.V. Coelho, A.V. Xavier, M. Teixeira, C.M. Soares, I.A.C. Pereira, Hydrogenases in *Desulfovibrio vulgaris* Hildenborough: structural and physiologic characterisation of the membrane-bound [NiFeSe] hydrogenase, J. Biol. Inorg. Chem. 10 (2005) 667–682.
[149] C. Baltazar, V. Teixeira, C. Soares, Structural features of [NiFeSe] and [NiFe] hydrogenases determining their different properties: a computational approach, J. Biol. Inorg. Chem. 17 (2012) 543–555.
[150] O. Rüdiger, C. Gutiérrez-Sánchez, D. Olea, I.A.C. Pereira, M. Vélez, V.M. Fernández, A.L. DeLacey, Enzymatic anodes for hydrogen fuel cells based on covalent attachment of Ni–Fe hydrogenases and direct electron transfer to SAM-modified gold electrodes, Electroanalysis 22 (2010) 776–783.
[151] M. Rousset, Y. Montet, B. Guigliarelli, N. Forget, M. Asso, P. Bertrand, J.C. Fontecilla-Camps, E.C. Hatchikian, [3Fe–4S] to [4Fe–4S] cluster conversion in *Desulfovibrio fructosovorans* [NiFe] hydrogenase by site-directed mutagenesis, Proc. Natl. Acad. Sci. U. S. A. 95 (1998) 11625.
[152] O.A. Zadvornyy, J.E. Lucon, R. Gerlach, N.A. Zorin, T. Douglas, T.E. Elgren, J.W. Peters, Photo-induced H_2 production by [NiFe]-hydrogenase from *T. roseopersicina* covalently linked to a Ru(II) photosensitizer, J. Inorg. Biochem. 106 (2012) 151–155.
[153] K.A. Vincent, J.A. Cracknell, J.R. Clark, M. Ludwig, O. Lenz, B. Friedrich, F.A. Armstrong, Electricity from low-level H2 in still air — an ultimate test for an oxygen tolerant hydrogenase, Chem. Commun. (2006) 5033–5035.
[154] S.L.A. Andrade, J.J.G. Moura, Hydrogen evolution and consumption in AOT-isooctane reverse micelles by *Desulfovibrio gigas* hydrogenase, Enzyme Microb. Technol. 31 (2002) 398–402.
[155] T.V. Tikhonova, S.A. Kurkin, N.L. Klyachko, V.O. Popov, Use of a reverse micelle system for study of oligomeric structure of NAD(+)-reducing hydrogenase from *Ralstonia eutropha* h16, Biochem. Mosc. 70 (2005) 645–651.

[156] A. Pandey, A. Pandey, P. Srivastava, A. Pandey, Using reverse micelles as microreactor for hydrogen production by coupled systems of Nostoc/R-palustris and Anabaena/R-palustris, World J. Microbiol. Biotechnol. 23 (2007) 269–274.
[157] H. Krassen, A. Schwarze, B. Friedrich, K. Ataka, O. Lenz, J. Heberle, Photosynthetic hydrogen production by a hybrid complex of photosystem I and [NiFe]-hydrogenase, ACS Nano 3 (2009) 4055–4061.
[158] A. Tiwari, A. Pandey, Cyanobacterial hydrogen production — a step towards clean environment, Int. J. Hydrogen Energy 37 (2012) 139–150.
[159] A. Singh, K. Misra, Improved hydrogen production by coupled systems of hydrogenase negative photosynthetic bacteria and fermentative bacteria in reverse micelles, Int. J. Hydrogen Energy 33 (2008) 6100–6108.
[160] B. Friedrich, J. Fritsch, O. Lenz, Oxygen-tolerant hydrogenases in hydrogen-based technologies, Curr. Opin. Biotechnol. 22 (2011) 358–364.
[161] C.E. Lubner, R. Grimme, D.A. Bryant, J.H. Golbeck, Wiring photosystem I for direct solar hydrogen production, Biochemistry 49 (2009) 404–414.
[162] C.E. Lubner, P. Knörzer, P.J.N. Silva, K.A. Vincent, T. Happe, D.A. Bryant, J.H. Golbeck, Wiring an [FeFe]-hydrogenase with photosystem I for light-induced hydrogen production, Biochemistry 49 (2010) 10264–10266.
[163] C.E. Lubner, A.M. Applegate, P. Knörzer, A. Ganago, D.A. Bryant, T. Happe, J.H. Golbeck, Solar hydrogen-producing bionanodevice outperforms natural photosynthesis, Proc. Natl. Acad. Sci. 108 (2011) 20988–20991.
[164] B.E. Barton, C.M. Whaley, T.B. Rauchfuss, D.L. Gray, Nickel–iron dithiolato hydrides relevant to the [NiFe]-hydrogenase active site, J. Am. Chem. Soc. 131 (2009) 6942–6943.
[165] A. Dutta, G.A. Hamilton, H.E. Hartnett, A.K. Jones, Construction of heterometallic clusters in a small peptide scaffold as [NiFe]-hydrogenase models: development of a synthetic methodology, Inorg. Chem. 51 (2012) 9580–9588.
[166] K. Weber, T. Krämer, H.S. Shafaat, T. Weyhermüller, E. Bill, M. van Gastel, F. Neese, W. Lubitz, A functional [NiFe]-hydrogenase model compound that undergoes biologically relevant reversible thiolate protonation, J. Am. Chem. Soc. 134 (2012) 20745–20755.
[167] M. Rakowski DuBois, D.L. DuBois, The roles of the first and second coordination spheres in the design of molecular catalysts for H_2 production and oxidation, Chem. Soc. Rev. 38 (2009) 62–72.
[168] M.E. Carroll, B.E. Barton, D.L. Gray, A.E. Mack, T.B. Rauchfuss, Active-site models for the nickel–iron hydrogenases: effects of ligands on reactivity and catalytic properties, Inorg. Chem. 50 (2011) 9554–9563.
[169] H.S. Shafaat, K. Weber, T. Petrenko, F. Neese, W. Lubitz, Key hydride vibrational modes in [NiFe] hydrogenase model compounds studied by resonance Raman spectroscopy and density functional calculations, Inorg. Chem. 51 (2012) 11787–11797.
[170] T.W. Muir, D. Sondhi, P.A. Cole, Expressed protein ligation: a general method for protein engineering, Proc. Natl. Acad. Sci. U. S. A. 95 (1998) 6705–6710.
[171] T.R. Ward, Artificial metalloenzymes based on the biotin–avidin technology: enantioselective catalysis and beyond, Acc. Chem. Res. 44 (2011) 47–57.
[172] Y. Lu, N. Yeung, N. Sieracki, N.M. Marshall, Design of functional metalloproteins, Nature 460 (2009) 855–862.
[173] P.J. Deuss, R. den Heeten, W. Laan, P.C.J. Kamer, Bioinspired catalyst design and artificial metalloenzymes, Chem. Eur. J. 17 (2011) 4680–4698.